THE CONVERSE PIEZOELECTRIC EFFECT IN WOOD AND CELLULOSE MATERIALS

Master Thesis

Submitted by
Johannes Plackner

Supervisor: Ao. Univ. Prof. DI Dr. Wolfgang Gindl

Institute of Wood Science and Technology
Department of Material Sciences and Process Engineering
University of Natural Resources and Applied Life Sciences
BOKU – Vienna

September 2009

Ich möchte meine Diplomarbeit einerseits meinen Eltern Gertraud und Franz widmen, die mich seit jeher in meinem Bildungsweg nach Kräften unterstützt haben und mir ein Fundament aus Neugier und Wissbegier gelegt haben. Andererseits sei sie meiner lieben Doris gewidmet, die ganz kräftig dazu beigetragen hat, dass meine Studentenzeit einfach großartig war.

Abstract

Wood and crystalline cellulose materials are known for exhibiting piezoelectric behavior. The direct piezoelectric effect (formation of an electric field along the surface when exposing to mechanical stress) is well researched. The converse piezoelectric effect, the change of mechanical properties due to application of an electric field was, however, never the aim of comprehensive research.

Two materials were investigated, native wood and regenerated cellulose. The wood samples were cut from pine wood blocks and measured 0,2x8x80 mm. The cellulose samples had the same dimensions. They were obtained from cellulose foils produced by partly dissolving highly crystalline cellulose powder with dimethylacetamide. To orient the fibers, the foils were stretched before testing. The samples have been analyzed by the means of conventional stress measurement to quantify the piezoelectric response and by wide angle x-ray scattering (WAXS) to understand the underlying principles.

The results showed a clear mechanical reaction on the electric field for wood, and a smaller, yet detectible reaction for the cellulose foils. For wood, the WAXS data indicated widening of the cellulose molecules within the crystallite. The cellulose samples didn’t show any response during the WAXS experiments.

Zusammenfassung

Es ist bekannt, dass Holz und Zellulose piezoelektrisch aktive Materialien sind. Der direkte Piezoeffekt (Aufbau eines elektrischen Feldes an der Oberfläche bei mechanischer Belastung) ist gut erforscht. Der indirekte Piezoeffekt, die mechanischen Veränderungen aufgrund des Anlegens eines elektrischen Feldes, wurde bislang nur wenig analysiert.

Im Zuge dieser Arbeit wurden zwei Materialien untersucht, Kiefernholz und Regeneratszellulose mit den Abmessungen 0,2x8x80 mm. Die Zelluloseproben wurden hergestellt, indem hochkristallines Zellulosepulver in Dimethylacetamid teilweise aufgelöst, ausgefällt und anschließend verstreckt wurde. Mittels einer Universalprüfmaschine wurde der Piezoeffekt quantifiziert. Weiters wurden die Materialien per wide angle x-ray scattering (WAXS) untersucht, um Aufschluss über Veränderungen im Kristallgitter zu erhalten.

Die Ergebnisse zeigen einen klaren indirekten piezoelektrischen Effekt bei den Holzproben und einen kleineren, doch messbaren Effekt bei den Zellulosefolien. Die WAXS Ergebnisse deuten auf eine Aufweitung des Zellulosekristalls hin.

Keywords: piezoelectric effect, wood, cellulose, piezoelectric texture

List of Figures

List of Tables

1. Introduction

1.1. Problem Description

Wood is a fascinating material. From its yet unveiled chemical mysteries in the very tiniest ultrastructural units to its majestic appearance in adult trees, it offers interesting aspects for scientific research. Often this research means nothing more than exposure of wood to a defined environment or influence and observing its reaction. Subsequently a scientist tries to develop a hypothesis that explains that reaction, accompanied by further experiments longing to verify or to decline that hypothesis.

The scientific work carried out by the author of this master thesis follows this very approach. The effect that shall be described herein is the mechanical reaction to an electric field. Although there was never sufficient evidence at hand, this was referred for decades to the piezoelectric effect in wood. In 1880 the first paper on the piezoelectric effect was published by Pierre and Jacques Curie (according to Benes, 2009). It was found that various crystals showed an electric polarization when mechanical stress was applied. These crystals included even cane sugar.

So from the very beginning of research in the piezoelectric effect, crystalline bio-materials were known to be able to demonstrate electro-mechanical behavior. Cellulose is also a natural matter showing the essential characteristics enabling the piezoelectric effect. Native cellulose, as opposed to manmade regenerated cellulose, shows a high crystallinity.

Table 1 gives an overview of the crystallinity of cellulose according to its origin. Since wood itself is a composite of mainly cellulose, hemi-cellulose and lignin, it seems logical that an electro-mechanic behavior will occur, even if it is alleviated compared to monocrystals.

As for many crystal materials, there is more than only one crystal lattice, cellulose crystals can compose (Kölln, 2004). Two of the most important crystalline states, cellulose I which occurs in plants, and cellulose II which occurs in regenerated cellulose will be investigated.

As to be demonstrated in the literature review, the piezoelectric behavior of wood was already of some interest to research teams around the world. But still there are large fields of the piezoelectric effect that have not yet been sufficiently researched. Especially for the converse piezoelectric effect in wood, only a few experiments have been carried out, yet (Bazhenov, 1961).

Table 1: Crystallinity of cellulose in regard to its origin. (Klemm, Heublein, Fink, & Bohn, 2005)

Cellulose Source	**Crystallinity [%]**
Algae Cellulose	> 80
Bacteria Cellulose	65-79
Cotton-Linters	56-65
Ramie	44-47
Flax	56
Hemp	59
Wooden Pulp	43-56

So the problem description for this thesis can be outlined as following:

1. Develop experiments that are suitable for measuring the converse piezoelectric effect in wood and cellulose materials.
2. Assess the piezoelectric effect in regard to certain parameters.
3. Based on these findings, try to explain the underlying mechanisms that caused this mechanic reaction on an electric field.

1.2. Possible Applications

Although this thesis follows the very approach of fundamental research, some possible, though not concrete applications, should be mentioned. The direct piezoelectric effect might be useful for non-destructive testing (e.g. see (Pizzi & Knuffel, 1986)) of wood since measurable electrical signals are generated when exposing the wood to a certain mechanical load. Since this effect is reversible, a better understanding of the converse piezoelectric effect can also lead to a more comprehensive knowledge of the direct piezoelectric effect.

2. Literature Review

2.1. Initial Discovery of the Piezoelectric Effect in Wood

Research in piezoelectricity of wood has been carried out around the globe, in institutes distributed over several continents. The oldest reference available referring to scientific work about the piezoelectric effect specifically was a paper from 1940[1]. It is cited in the book “Piezoelectric Properties of Wood” by the Soviet researcher Valerie A. Bazhenov (Bazhenov, 1961).

2.1.1. Eiichi Fukada, Japan, 1955

In 1955 a paper titled “Piezoelectricity of Wood” was published in Japan by the scientist Eiichi Fukada (Fukada, 1955). It is the oldest source available as full-text in English. He analyzed both, the direct and the converse piezoelectric effect in wood. The first one was being characterized by applying stress to a piece of wood. Since it was already supposed, that the piezoelectric effect in wood is caused by shear strain; the wood specimen’s grain had a 45° angle in respect to the applied force. Figure 1 shows a schematic draft of the device.

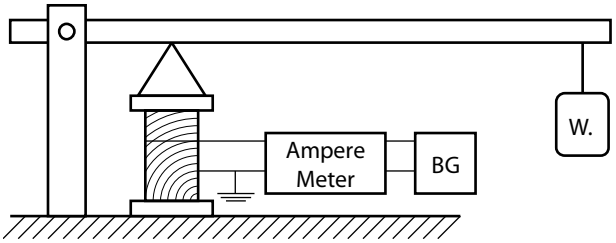

Figure 1: Schematic draft of the device used by Fukada, 1955 to measure the direct piezoelectric effect. (BG - ballistic galvanometer, W. - Weight)

Fukada also proved the existence of the converse piezoelectric effect. A device was crafted that had two active parts: a wooden specimen with a 45° grain angle and a Rochelle salt crystal. The assumption was that the wooden specimen would start to vibrate when exposed to an oscillating electric field. The mechanic reaction was recorded by the Rochelle salt crystal that is known to have strong piezoelectricity.

Results showed that there was a strong correlation between the applied current on the wood and output current from the Rochelle salt crystal. Since both, wood and crystal, were insulated from each other and any environmental effect could

[1] A. V. Shubnikov: On the tensor piezoelectric moduli of noncrystalline anisotropic media, Report in the Division of Phyiskal-Mathematical Sciences of the Academy of Sciences of the USSR, April 25th, 1940

be excluded this was a valid proof of the direct piezoelectric effect in wood. Subsequently, Fukada calculated from the measurements the piezoelectric constants of the investigated materials.

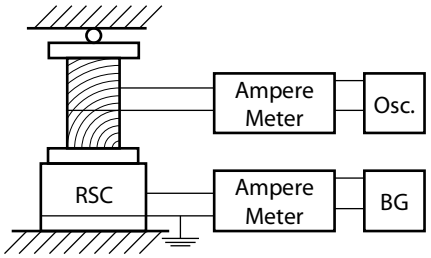

Figure 2: Schematic draft of the device used by Fukada, 1955 to measure the converse piezoelectric effect. (RSC - Rochell salt crystal; BG - ballistic galvanometer, Osc. - Oscillator)

Table 2: Piezoelectric constants determined by Fukada (extract from (Fukada, 1955))

	Piezoelectric Constant	
Material	direct	converse
maple	$-2.6 \cdot 10^{-9}$	$-2.4 \cdot 10^{-9}$
spruce	$-5.0 \cdot 10^{-9}$	$-2.3 \cdot 10^{-9}$
ash	$-6.2 \cdot 10^{-9}$	$-8.0 \cdot 10^{-9}$

2.1.2. Valerie A. Bazhenov, USSR, 1962

In 1959, the above mentioned Soviet scientist Valerie A. Bazhenov authored the book ‘Piezoelectric Properties of Wood’. It is a comprehensive collection and connection of knowledge in wood science, piezoelectricity and the findings from Shubnikov and Fukada. Also, considerable experiments were conducted with a special focus to better describe the magnitude of the piezoelectric effect.

Although there was no definitive evidence at that time, it was supposed, that cellulose molecules might be the cause for the shown phenomena. This conclusion is necessary since wood pulp that consists almost exclusively of cellulose seemed to feature piezoelectricity, too. But besides that, it was not clear what exactly the basic unit in the wood is that causes piezoelectricity. Bazhenov named it the “nucleus” of the piezoelectric effect and recommended to focus further research in that area. The exact citation is (Bazhenov, 1961, p 131):

"The foregoing has served to set out the fundamental tasks of our future investigations:

1. *To find the smallest particle that is capable of imparting piezoelectric properties to all cellulose materials:*
2. *To establish the piezoelectric properties of the larger particles of cellulose materials – the fibrils and cells;*
3. *To examine the piezoelectric properties of wood as a texture made up of differentiated cells grouped together in the basic tissues;*
4. *To explain, as the result of the analytic solution of the above problems, the features of wood as a piezoelectric texture that have made their appearance in the experimental study of the piezoelectric properties of individual species."*

2.1.3. William L. Galligan and Larry D. Bertholf, USA, 1963

The starting point for Galligan's and Bertholf's research work ('Piezoelectric Effect in Wood') was the goal to develop a new approach for non-destructive testing of adhesive bonds in long wood specimens. Therefore he built an apparatus that caused a shock-wave along the length of the specimen by impacting the front end of a beam.

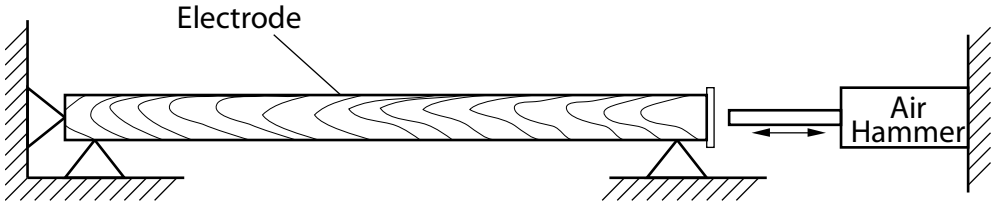

Figure 3: Apparatus used by Galligan and Bertholf to create a shock-wave throughout the long wood specimen and an electrode detecting an electric field along the surfaces (Galligan & Bertholf, 1963).The specimen was made from Douglas fir wood and measured ¾-inch by ¾-inch by 30-inch.

For detecting an electric signal caused by a piezoelectric effect, an electrode was put along the surfaces without actually touching it. This electrode was moved along the circumference, measuring the piezoelectric voltage in 6 points per side, 24 in total. This measurement was carried out for several distances from the impact point.

Results showed a clear electrical signal (several millivolts) especially close to the impact point. In particular, the charge distribution is of interest. Galligan and Bertholf were able to define a specific positive or negative charge, depending on the grain (Figure 4). Hence, occurrences that cause grain deviations (like

knots) could influence the polarity of the surfaces or, more exact, the localization of the point of zero volts.

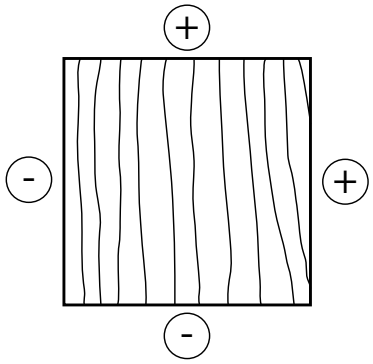

Figure 4: Generalization of the polarity observed in the piezoelectric effect caused by a stress-wave in long wood specimens (Galligan & Bertholf, 1963).

A further focus was put upon the influence of density and wood defects on the piezoelectric effects. Both were found to affect the electric response and it was possible to identify knots by analyzing the exact position of the zero-voltage point along the surface.

2.1.4. P. W. Kelso, USA, 1969

Based on Bertholf and Galligan's findings, a master thesis was carried out two years later at the same institution (Washington State University, Pullman, USA) by Paul W. Kelso (Kelso, 1969). In this thesis he summed up the findings in this field of research at that time. Fukada and Bazhenov tried to develop a tensor relation between that explains the piezoelectric behavior of wood. Assuming that the wood structure is an orthorhombic system, Hooke's law can be shown in matrix form as:

$$\begin{bmatrix}\varepsilon_{11}\\ \varepsilon_{22}\\ \varepsilon_{33}\\ \varepsilon_{23}\\ \varepsilon_{31}\\ \varepsilon_{12}\end{bmatrix} = \begin{bmatrix} c_{11} & c_{12} & c_{13} & & & \\ c_{21} & c_{22} & c_{23} & & & \\ c_{31} & c_{32} & c_{33} & & & \\ & & & c_{44} & & \\ & & & & c_{55} & \\ & & & & & c_{66}\end{bmatrix} \cdot \begin{bmatrix}\sigma_{11}\\ \sigma_{22}\\ \sigma_{33}\\ \sigma_{23}\\ \sigma_{31}\\ \sigma_{12}\end{bmatrix}$$

From these basic mechanical relations it is possible to develop an equation that explains the piezoelectric behavior of wood. The amplitude of the piezoelectric response is given by a polarization vector. Bazhenov assumes a linear relation between the components of the polarization vector and the components of stress or mechanical strain (Bazhenov, 1961). For the case of stresses, this relation may be expressed as:

$$\begin{bmatrix} P_1 \\ P_2 \\ P_3 \end{bmatrix} = \begin{bmatrix} d_{11} & d_{12} & d_{13} & d_{14} & d_{15} & d_{16} \\ d_{21} & d_{22} & d_{23} & d_{24} & d_{25} & d_{26} \\ d_{31} & d_{32} & d_{33} & d_{34} & d_{35} & d_{36} \end{bmatrix} \cdot \begin{bmatrix} \sigma_{11} \\ \sigma_{22} \\ \sigma_{33} \\ \sigma_{23} \\ \sigma_{31} \\ \sigma_{12} \end{bmatrix}$$

P is the component of the piezoelectric vector and d is the component of the piezoelectric tensor called a piezoelectric stress constant. This is the most general piezoelectric/stress relation. For wood, certain assumptions can be made that simplifies that tensor. Fukada recognized the monoclinic characteristic of the cellulose crystal in wood and derived the following tensor (valid for the cellulose I unit cell; indices *1, 2, 3* correspond to the *a, c, b* direction in the unit cell → Figure 14):

$$\begin{bmatrix} P_1 \\ P_2 \\ P_3 \end{bmatrix} = \begin{bmatrix} 0 & 0 & 0 & d_{14} & d_{15} & 0 \\ 0 & 0 & 0 & d_{24} & d_{25} & 0 \\ d_{31} & d_{32} & d_{33} & 0 & 0 & d_{36} \end{bmatrix} \cdot \begin{bmatrix} \sigma_{11} \\ \sigma_{22} \\ \sigma_{33} \\ \sigma_{23} \\ \sigma_{31} \\ \sigma_{12} \end{bmatrix}$$

Subsequently Fukada made the following assumptions (Fukada, 1955):

- the microfibrils are oriented parallel to the *1* axis
- the microfibrils are oriented so that their axes are parallel to each other but the polarity of the axes is at random
- a and c axis of the crystals are distributed evenly at random in the *1,2* plane
- random-distribution of the b axis

With these assumptions the d_{31}, d_{32}, d_{33}, d_{15}, and d_{24} components are cancelled and disappear. What is left remaining is a theoretical piezoelectric tensor (valid for the whole system) of

$$\begin{bmatrix} P_1 \\ P_2 \\ P_3 \end{bmatrix} = \begin{bmatrix} 0 & 0 & 0 & d_{14} & 0 & 0 \\ 0 & 0 & 0 & 0 & d_{25} & 0 \\ 0 & 0 & 0 & 0 & 0 & 0 \end{bmatrix} \cdot \begin{bmatrix} \sigma_{11} \\ \sigma_{22} \\ \sigma_{33} \\ \sigma_{23} \\ \sigma_{31} \\ \sigma_{12} \end{bmatrix}$$

This tensor form matches with experimental data obtained from Fukada and Bazhenov. Those experiments mostly showed the direct piezoelectric effect in a shear direction. These results were supported by the theoretical tensor mathematics.

Furthermore the influence of several wood characteristics (moisture content, pitch pockets, fiber orientation, growth rings) on the direct piezoelectric effect of wood was presented. The underlying aim was to develop a new method of non-destructive testing of structural wood elements. This was, as the further technical development showed, not realized by using a piezoelectric probe, but with means of x-rays, ultrasonic sound and visual analysis systems.

2.2. Further development

2.2.1. A. Pizzi and N Eaton, 1984, South Africa

Pizzi and Eaton (‘Correlation between the Molecular Forces in the Cellulose I Crystal and the Piezoelectric Effect in Wood') tried to find an explanation on the molecular level for the piezoelectric effect of wood. Based on Bazhenov’s findings, they used conformation analysis to investigate the forces that are responsible for the piezoelectric effect. Five different shear deformations of a Cellulose I were applied and the energy variations of Van-der-Waals, H-bond and electrostatic interactions were determined. According to his findings, only Van-der-Waals interactions are the cause for the piezoelectric effect.

2.2.2. A. Pizzi and W. Knuffel, 1986 and 1988, South Africa

In two consecutive published papers (‘Part I: The Piezoelectric Effect in Structural Timber’) Pizzi and Knuffel, respectively, analyzed the piezoelectric effect in structural timber. The principle of the measurements and the design of the experiments were rather similar to those carried out by Galligan and Bertholf, 1963, but with more sophisticated apparatuses and measurement devices. Besides the confirmation of the findings of Galligan and Bertholf, Pizzi and Knuffel focused on the influence of the moisture content on the amplitude of the piezoelectric effect.

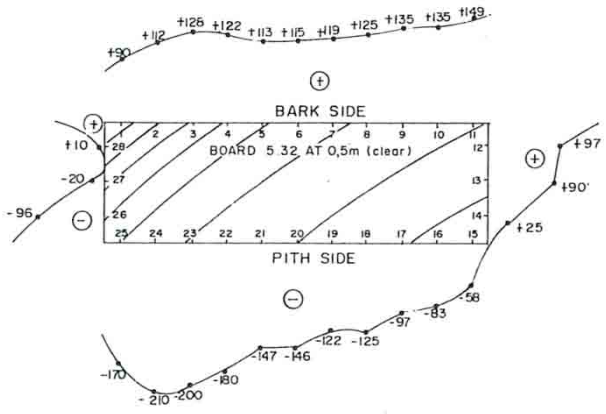

Figure 5: Direct piezoelectric effect measured by (Pizzi & Knuffel, 1986). The results are in accordance with Galligan and Bertholf (see Figure 4) but with a better resolution of measurement.

The second paper ('Part II: The Influence of Natural Defects') issued in 1988, dealt in particular with the relationship of the piezoelectric effect, the modulus of elasticity (MOE) and the occurrence of knots. In order to investigate this, 3.3 by 0.1 by 0.034 m measured boards were impacted with a cam-driven pendulum hammer to induce a shock-wave throughout the specimen. By measuring the voltage along the surface, it was possible to draw a two dimensional piezoelectric profile and compare it with the occurrence of knots (shown in Figure 6) and the measured MOE, respectively.

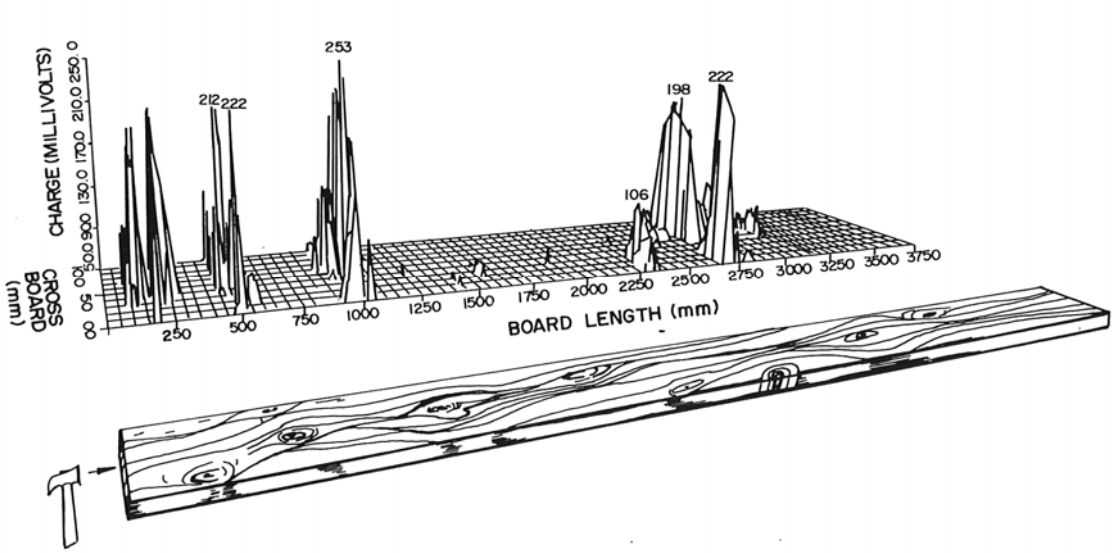

Figure 6 (Pizzi & Knuffel, 1986): The piezoelectric response on a shockwave and the occurrences of knots in the according board (pine, 34 x 100mm cross section)

2.3. Recent research activities

2.3.1. Peter Niemz et al., 1994, Germany

This research group in Germany tried to use the piezoelectric signal caused by drying tension in lumber to determine the moisture content. The internal stress occurring in a wooden board during the measurement could lead to a detectable electric field. Based on the following relationship they tried to calculate the moisture content from the piezoelectric modulus[2].

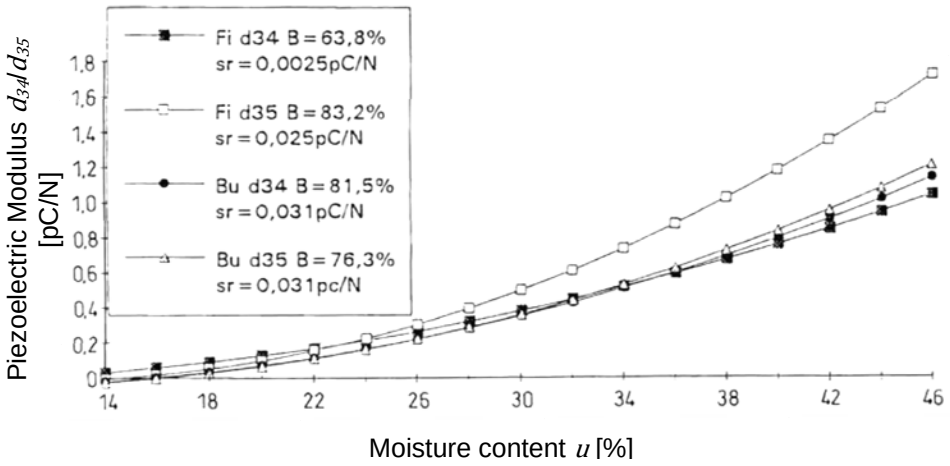

Figure 7: Effect of moisture content on the piezoelectric properties caused by mechanical stimulation of spruce (Fi) and beech (Bu) wood (Niemz, Emmler, Pridöhl, Fröhlich, & Lühmann, 1994).

The experiments showed that the piezoelectric signal was obliterated by considerable noise. It was, however, possible to observe signals that clearly relate to internal stress due to drying.

2.3.2. Takahisa Nakai, et al., 1998, Japan

Starting in 1990 most research related to the piezoelectric effect in wood was carried out in Japan. After publishing three articles in Japanese, the above mentioned researchers issued a paper in English dealing with the 'Piezoelectric behavior of wood under combined compression and vibration stresses'. The focus of that work was on the relation between piezoelectric behavior and the deformation of tracheids under combined compression and vibration stresses.

The results showed that two different kinds of breaking mechanisms are apparent. With the first case the tracheids broke only by shearing fracture in a 45° angle. In the second case, the specimens were finally broken by shearing

[2] The piezoelectric modulus [m/V] is a tensor describing the deflection of the material exposed to an electric field.

fracture after repeated buckling. In both cases a clear piezoelectrical signal could be measured and a linear relationship between the piezoelectric parameter and the Young's modulus could be calculated. An interesting reference is an older article in Japanese that concluded a piezoelectric effect in wood disappeared with moisture content higher than 6%. This is clearly opposite to what Knuffel and Pizzi (1986) published.

2.3.3. Jaehwan Kim, Sungryul Yun and Zoubeida Ounaies, 2006, USA

The Korean and American researchers, respectively, published a paper ('Discovery of Cellulose as a Smart Material) that focused on using cellulose as electro active paper (EAPap); a material that would show mechanical reaction on an electric field, similar to what the piezoelectric effect represents. The material used consisted of cellulose II crystals, covered by gold electrodes.

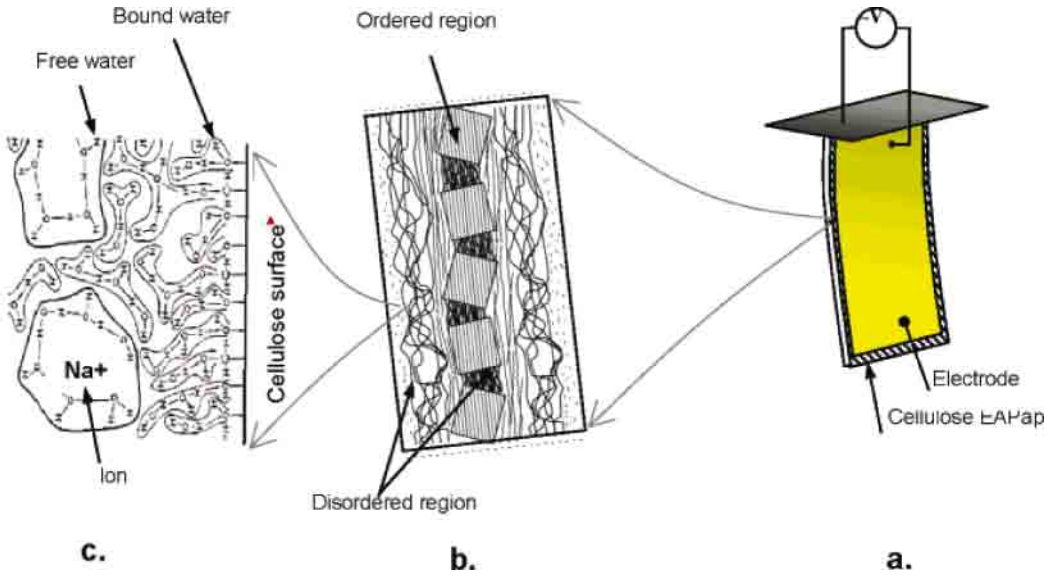

Figure 8: Concept of the electro active actuator. (a) cellulose microfibril has ordered crystalline regions and disordered regions; (b) EAPap is made from cellulose paper on which gold electrodes are deposited on both sides; (c) water molecules are bonded with hydroxyls on the cellulose surface (bound water) or clustered in free (free water) (Kim, Yun, & Ounaies, 2006).

Kim et al. applied further X-ray diffraction and thermally stimulated current measurement to understand the concept of the actuation phenomenon. They suspected two underlying mechanisms to be responsible: ion migration and dipolar orientation. Although they mentioned researchers like Bazhenov and Fukada in their introduction they did not follow the idea of a piezoelectric effect being the reason for the actuation.

2.4. Overview

Table 3: Overview of the relevant literature in the topic of piezoelectricity in wood.

Year/Author	***Title*/Content**
1952 E. Fukada	*Piezoelectricity of Wood:* Proof of both, the direct and the converse piezoelectric effect with experiments.
1962 V.A. Bazhenov	*Piezoelectric Properties of Wood:* Comprehensive analysis and quantification of basic and specific piezoelectric properties of wood. Extensive tensor mathematics.
1963 W. Galligan, L. Bertholf	*Piezoelectric Effect in Wood:* Analysis of the electric fields generated by a stresswave in structural timber. Attempts to find a relationship between the piezoelectric behavior and knots.
1969 P. W. Kelso	*Piezoelectric Effect in Wood (Master Thesis):* Kelso on developing a reliable and reproducible testing method for the direct piezoelectric effect in wood. He mainly focused on the findings of Galligan and Bertholf and tried to determine the effect of wood defects, grain, pitch and water content.
1984 A. Pizzi, N. Eaton	*Correlation between the Molecular Forces I the Cellulose I Crytal and the Piezoelectric Effect in Wood:* Investigation of the molecular forces causing the piezoelectric effect in wood.
1986 W. Knuffel, A. Pizzi	*The Piezoelectric Effect in Structural Timber:* Using an impact induced stress wave, the piezoelectric effect in structural timber was analyzed. A possible development of a stressgrading system or weakest point detection was assessed.
1988 W. Knuffel	*The Piezoelectric Effect in Structural Timber, Part II:* The effect of natural knots, cross grain, slope of grain and pith on the piezoelectric response was assessed.
1994 P. Niemz et al.	*Vergleichende Untersuchungen zur Anwendung von piezoelektrischen und Schallemissionssignalen bei der Trocknung von Holz:* Attempt to relate piezoelectric signals caused by internal drying stress to the actual moisture content.
1998 T. Nakai, N. Igushi, K. Ando	*Piezoelectric behavior of wood under combined compression and vibration stresses:* The relation of the piezoelectric behavior and the breakage of tracheids was analyzed by the means of on-time SEM.
2006 J. Kim, S. Yun, Z. Ounaies	*Discovery of Cellulose as a Smart Material:* A cellulose II foil is exposed to an electrical dc field. The apparent actuation was characterized.

3. The Piezoelectric Effect

3.1. Basic principles

The direct piezoelectric effect refers to the creation of an electric field along a crystalline structure's surface by applying mechanical stress. That effect is only shown by non-conductive materials, which means that no electric current is actually flowing. It is caused by a shift of the displacement in the crystal's ions, compared to the unloaded state. This entails in a shift of charges that accumulates over all displaced ions, hence it can be macroscopically measured, as an electric current between the opposite sides of the crystallite's surface (Benes, 2009).

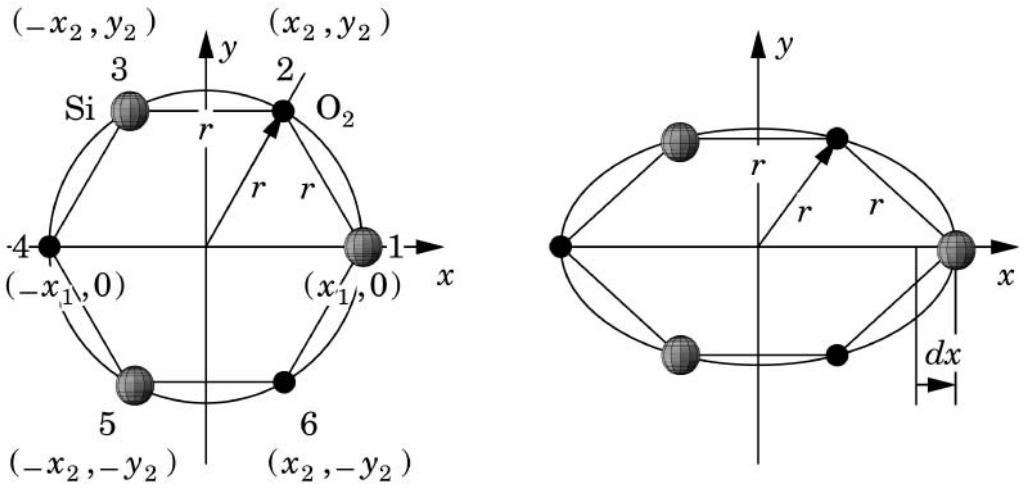

Figure 9: Plane model of the unit cell of an α-quartz crystal without (left) and with (right) applied tensile stress in the *x*-direction (Benes, 2009)

The application of mechanic stress results, according to Hooke's law, in a deformation of the material. A crystal is characterized by a long-range order of atoms. That means that a displacement on the crystal's surface is equally distributed to every spot in the lattice, influencing the ions that have a defined position.

Figure 9 shows a quartz crystal layer with Si and O_2 atoms. Applying stress in the direction of the y-axis results in a deformation of the crystal's profile while the interspace between the ions persists. If the crystal is non-symmetric in regard to the direction of the load (in Figure 9 this is along the y-axis), the displacement of atoms (dx) is equipollent to a shift of the charge distribution. Hence, the direct piezoelectric effect results in an electrical field, generated by a homogeneous displacement of crystal atoms. One characteristic feature of this

phenomenon is the reversibility – the application of an electrical field to a piezoelectric active crystal results in a deformation (see Figure 10) (Benes, 2009).

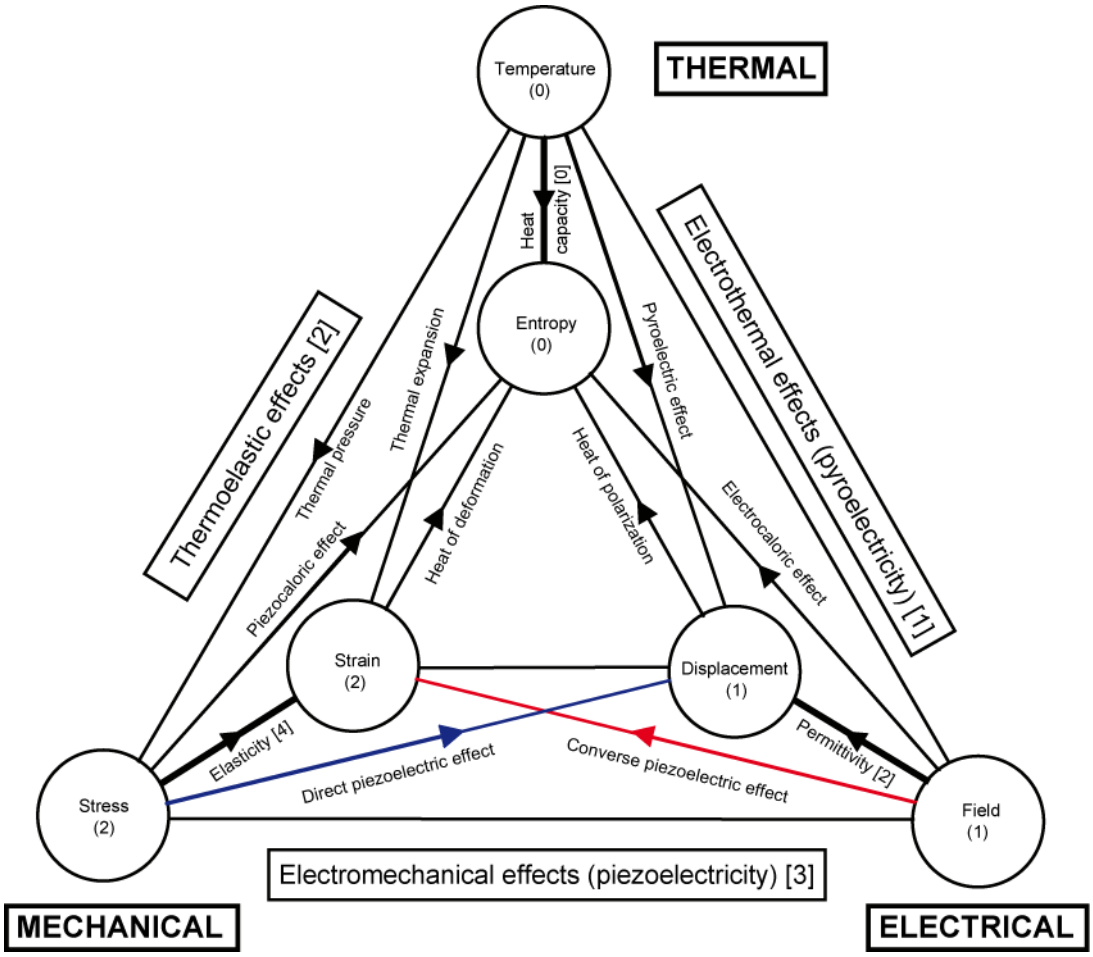

Figure 10: “The relations between the thermal, electrical and mechanical properties of a crystal, showing the names of the properties and the variables. The tensor rank of the variables is shown in round brackets and the tensor rank of the properties in square brackets.” (Benes, 2009) The effects that are decisive for this thesis (the direct and converse piezoelectric effects) are colored.

The relation between an applied field and the mechanic reaction can be expressed in following equation:

$$S_p = d_{ip} \cdot E_i$$

Whereas S_p is the strain, d_{ip}, the piezoelectric constant and E_i the applied electrical field. The first subscript to d indicates the direction of the polarization generated by the electrical field. The second subscript is the direction of the resulting strain (Benes, 2009). An example for the piezoelectric tensor of wood can be found in chapter 2.1.4.

3.2. Piezo Effect in cellulose materials

3.2.1. Composition of cellulose materials

Cellulose is the most common bio-polymer on earth since it is the main component of a plant's cell wall. It is a non-branched, threadlike molecule consisting of D-glucoses that are connected with an 1,4-glycosidic binding. The glucose molecules are twisted 180° to each other; hence the basic element of cellulose is a disaccharide (cellubiose), assembled by two twisted glucose molecules (Fengel & Wegener, 1989).

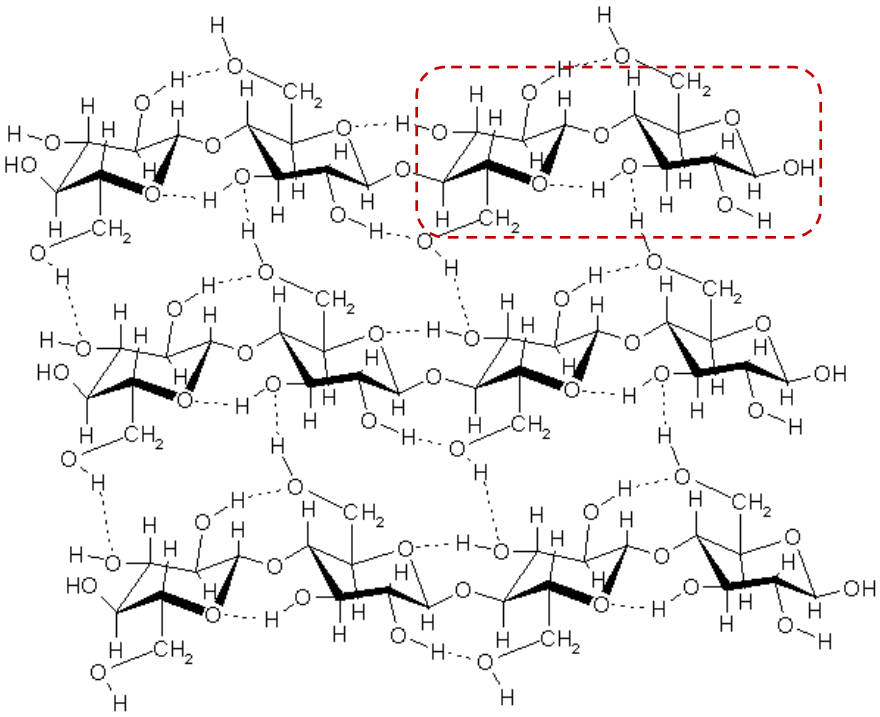

Figure 11: Intramolecular and intermolecular (dotted) hydrogen bonds in a cellulose molecule. Two 6-C glucose rings, twisted for 180°, create the basic cellubiose unit, as shown in the dashed red rectangle. (Greer & Pemberton, 2009)

These linear cellulose macromolecules are able to bear high tensile stress. Lignin, which is the second main component of wood, is an amorphous polymer that handles compression stress in a cell wall. These two molecules are interlocked by hemicelluloses, a polyose consisting of 5-C sugars. Cellulose is apparent in both, an amorphous and a crystal state (Kölln, 2004). Figure 12 shows a draft illustrating the entanglement of the cellulose from its very molecular units to the scope of cell walls.

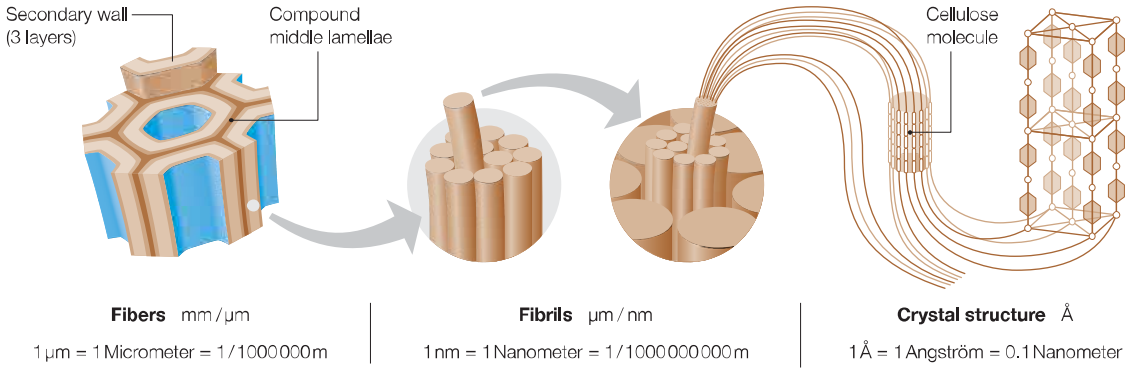

Figure 12: scheme of a wood cell wall showing the compound middle lamella (middle lamella and primary wall), and three layers of secondary wall. Cellulose, the principal component of the cell wall, exists as a system of fibrils. Parts of the fibrils are arranged in an orderly fashion and provide crystalline properties to the wall (Zimmermann, Pöhler, & Geiger, 2004).

The cellulose-crystal is currently known to exist in seven different polymorphs, of which only two can be assembled by nature, cellulose I_α and I_β. The ratio between cellulose I_α and I_β varies between species but also within a cell wall. Cellulose I_α is metastable and can be transformed into cellulose I_β by treatment with caustic soda. Besides the natural cellulose I, cellulose II is the most important of the polymorphs. It can be produced in two ways; either by hydrolysis of cellulose I by precipitation in an acidic bath or by mercerization in concentrated caustic soda (without actually dissolving the molecules). Cellulose II is widely used in industry and is known as Rayon or Viscose (Kölln, 2004). This thesis focuses on Cellulose I and cellulose II since the first one occurs in the wood and the latter in regenerated cellulose.

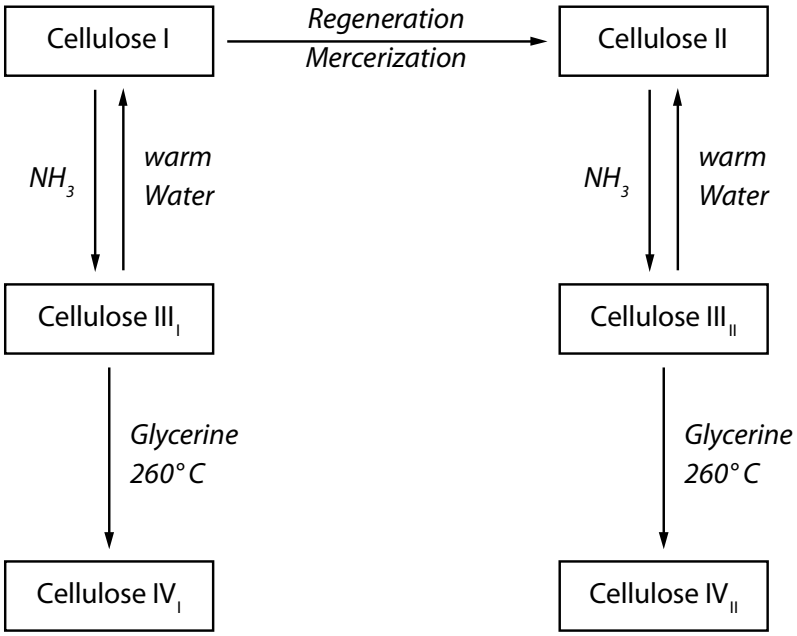

Figure 13: Conversion of the different cellulose polymorphs into each other (Kölln, 2004).

When it comes to the analysis of the piezoelectric effect in wood the exact structure of the crystal lattice is of interest. Table 4 and Figure 14 give the specifications for the mentioned polymorphs.

Table 4: Parameter of the unit cell of the cellulose polymorphs cellulose I_β and cellulose II (Kölln, 2004).

Species	**Cellulose I_β**	**Cellulose II**
Space group	Mononclinic	Monoclinic
a [Å]	7.784	8.10
b [Å]	8.201	9.03
c [Å]	10.380	10.31
α [°]	90	90
β [°]	90	90
γ [°]	96.5	117.10

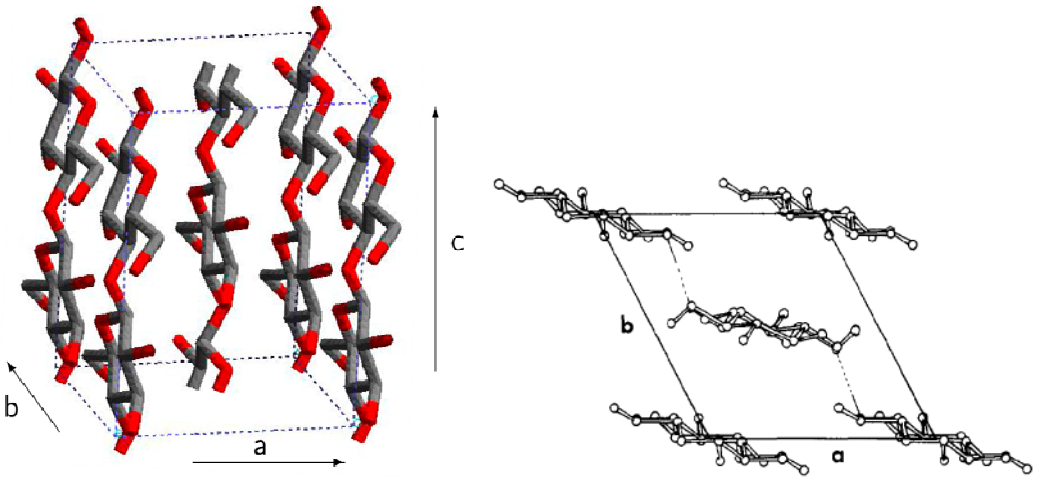

Figure 14: The unit cells of cellulose I_β (left) and cellulose II (right) (Kölln, 2004). In the cellulose I_β draft the axes are clearly visible, in the cellulose II draft the c-axis run parallel to the line of view.

Besides the particular composition of cellulose and its crystal states, the morphology of cellulose in wood has to be considered. The cellulose molecules are assembled in the cell wall and are responsible for bearing tensile loads. During the growth period of a cell wall, the load changes and the orientation of the cellulose in the cell wall does, as well.

The cellulose chains are embedded in an amorphous matrix consisting of lignin and hemi-celluloses. In terms of the piezoelectric behavior, this mixture of the crystalline[3] cellulose chains and the amorphous matrix can be identified as a piezoelectric texture. The proportion of cellulose, the degree of orientation of the cellulose chains and the degree of crystallinity will influence the mechanical response.

3.2.2. The piezoelectric texture in wood and regenerated cellulose

Besides the pure piezoelectric effect in monocrystals, electromechanical behavior can also be observed in "piezoelectric textures", a term defined by A.V. Shubkinov (Bazhenov, 1961). These textures consist merely of crystal aggregates. Those aggregates have to be oriented so that the axes of the several crystals are parallel or almost parallel. Wood- or cellulose-based materials contain those piezoelectric textures in the form of cellulose I or cellulose II crystals.

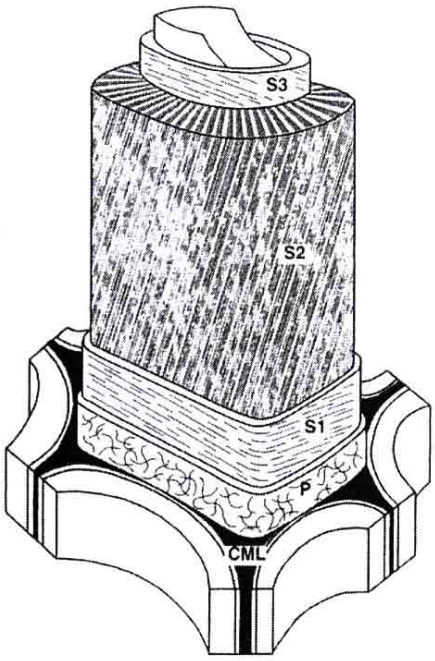

Figure 15: Cell wall model of wood (Fengel & Wegener, 1989). CML: compound middle lamella; P: primary wall; S1, S2, S3: layers of the secondary wall with different fiber orientation.

As shown in Figure 15, the cell wall's most decisive region is the S2 layer. That's where one finds well oriented cellulose microfibrils with a high degree of crystallinity. Hence, the S2 layer can be seen as a piezoelectric texture where

[3] Not all of the cellulose in the cell wall is in a crystal state.

Table 1 gives an overview of the crystallinity of cellulose depending on its origin.

the cellulose molucules wind helix-like around the cell void. So the microfibril-angle[4] has to be put in account when trying to explain piezoelectric behavior of wood.

[4] The microfibril angle describes the angle between the longitudinal axis of the cell and the direction of the cellulose micro fiber bundles.

4. Experimental Verification

4.1. Methods and Materials

4.1.1. Sample Preparation

4.1.1.1. Wood Samples

To allow an experimental detection of a piezoelectric effect in wooden samples, the specimens had to meet following specifications:

- It had to be possible to apply a strong electric field to the sample
- The field should penetrate the sample homogeneously
- The sample had to be large enough that a mechanic reaction could be observed

Following these conditions it was obvious that the samples had to be very thin, but able to be mounted on the universal testing machine and used for mechanical analysis.

4.1.1.1.1. Microtome cutting

For the wood samples Scotch Pine (*Pinus sylvestris*) was chosen because it shows a comparably high crystallinity of its cellulose[5]. Five different blocks (according to the five different fiber angles analyzed) of the pinewood were stored in water for several days to ease cutting. Using a microtome, 200µm thin wooden disks were sliced from the blocks. Figure 16 shows the shape of the wooden samples and the according fiber angles. After cutting, the samples were flattened with a hot iron; a process that also removed most of the contained water.

For easier handling and clamping in the universal testing machine, glue-veneer was attached on the ends of the samples. For each of the five fiber orientations, 30 samples were produced. The specimens were then stored in a controlled environment with a temperature of 20° C and 60% relative humidity.

[5] Bleached sulphate pulp from spruce containes cellulose with a crystallinity of 68%, from birch 65.1 %, from bamboo 59.9% (Fengel & Wegener, 1989)

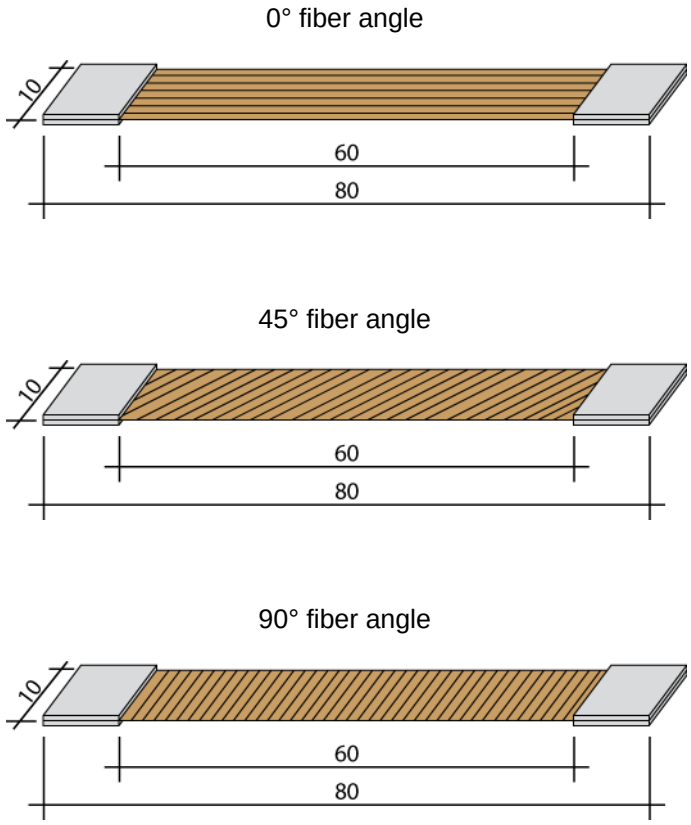

Figure 16: Shape of the wood samples (scale in mm) used for detecting the piezoelectric effect. The ends were attached to veneer for easier handling. The lines indicate three of the five different fiber angles.

4.1.1.1.2. Circular Saw Cutting

Especially for the 90° fiber angle, the microtome cutting turned out to be problematic. The unavoidable bending when the blade sliced through the wood destroyed or predamaged some of the samples. To produce suitable samples for comparing the piezoelectric response in respect to the fiber angle, an alternative technique was used. From a 50mm thick pine wood board, an only 0.2 mm thick sheet of wood was cut with a circular saw. Subsequently, from the resulting sheet 8 mm wide strips were cut, in a 0°, 45° and 90° angle.

4.1.1.1.3. Mechanical Characterization

Prior to the actual piezoelectric experiments 10 samples of each fiber orientation were mechanically tested to determine E-modulus and tensile strength. The results are displayed in Figure 17. The bold lines show the results for the 200 µm thick specimens. In respect to the logarithmic scales, the decrease in tensile strength is greater than expected. This was probably caused by structural damage within the specimens. This problem mainly occurred in specimens that possessed higher fiber angles. They were considerably more difficult to cut and did not have a perfectly planar surface. These imperfections

acted like a predetermined breaking point and reduced the tensile strength substantially. In order to increase or obtain proper sample size, new samples with the same specifications except a greater thickness of 2 mm were introduced for the 45°, 67.5° and 90° oriented specimens. These samples were prepared using a twin-blade circular saw as opposed to a microtome. The samples cut with the circular saw were not mechanically characterized prior to the piezoelectric experiments.

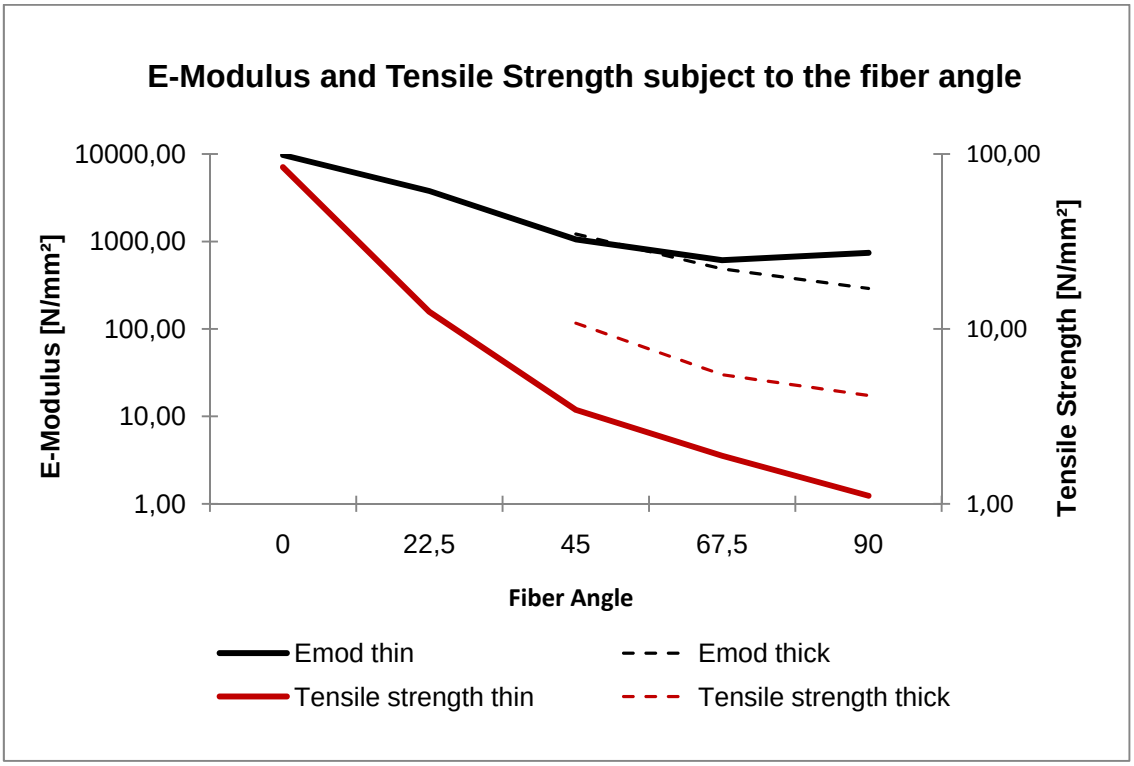

Figure 17: E-Modulus (Emod) and tensile strength subject to the fiber angle. The thin samples showed a strong decrease of their mechanic properties. So 2 mm thick samples were introduced to get proper data for 45°, 67,5° and 90°, orientations.

The thicker samples are marked with the thinner, dashed line. For the E-modulus, the 45° and the 67.5° sample lie within an acceptable deviation. The 90° samples show an E-modulus deviation with a factor 2.5 whereas the thin samples had an even higher value. The difference in regard to the tensile strength was more severe. There the deviation was already observable at a fiber angle of 45° (factor 3.1) and grew higher to the crossways oriented samples (factor 3.7) as shown in Table 5.

Table 5: E-moduli and tensile strengths of 0.2 and 2 mm thick wooden samples. Values are the mean of 10 specimens except for the 0.2 mm 67.5° and 90° samples where the number was 5.

	E-Modulus [N/mm²]		**Tensile strength [N/mm²]**	
Fiber Angle	0.2 mm	2 mm	0.2 mm	2 mm
0°	9739.82		84.04	
22.5°	3779.77		12.51	
45°	1058.07	1217.72	3.45	10.79
67.5°	611.33	486.61	1.88	5.47
90°	640.89	290.46	1.11	4.16

If one keeps in mind that the E-moduli are calculated from data gathered with a stress level well below the tensile strength it is obvious that the elasticity is not influenced by a predetermined breaking point. Hence, the observed differences between the 0.2 mm and the 2 mm specimens are not surprising.

4.1.1.1.4. Conductive Paint

The specimens destined for the piezoelectric tests subsequently needed to be given a conductive face. This was achieved by painting the surface with conductive silver-paint (Silber Leitlack 5900, Busch GmbH, Viernheim, Germany).

To determine how well the coverage of the samples was and how deep the silver paint penetrated the wooden matter, microscopic images were taken from a sample's cross section (Figure 18). It is obvious, that the silver paint is not distributed evenly across the surface. Also, the paint entered the wooden matter in cracks, but did not penetrate solid wood cells. The images might suggest that with a better coating of the surface, the electrical field might be even stronger.

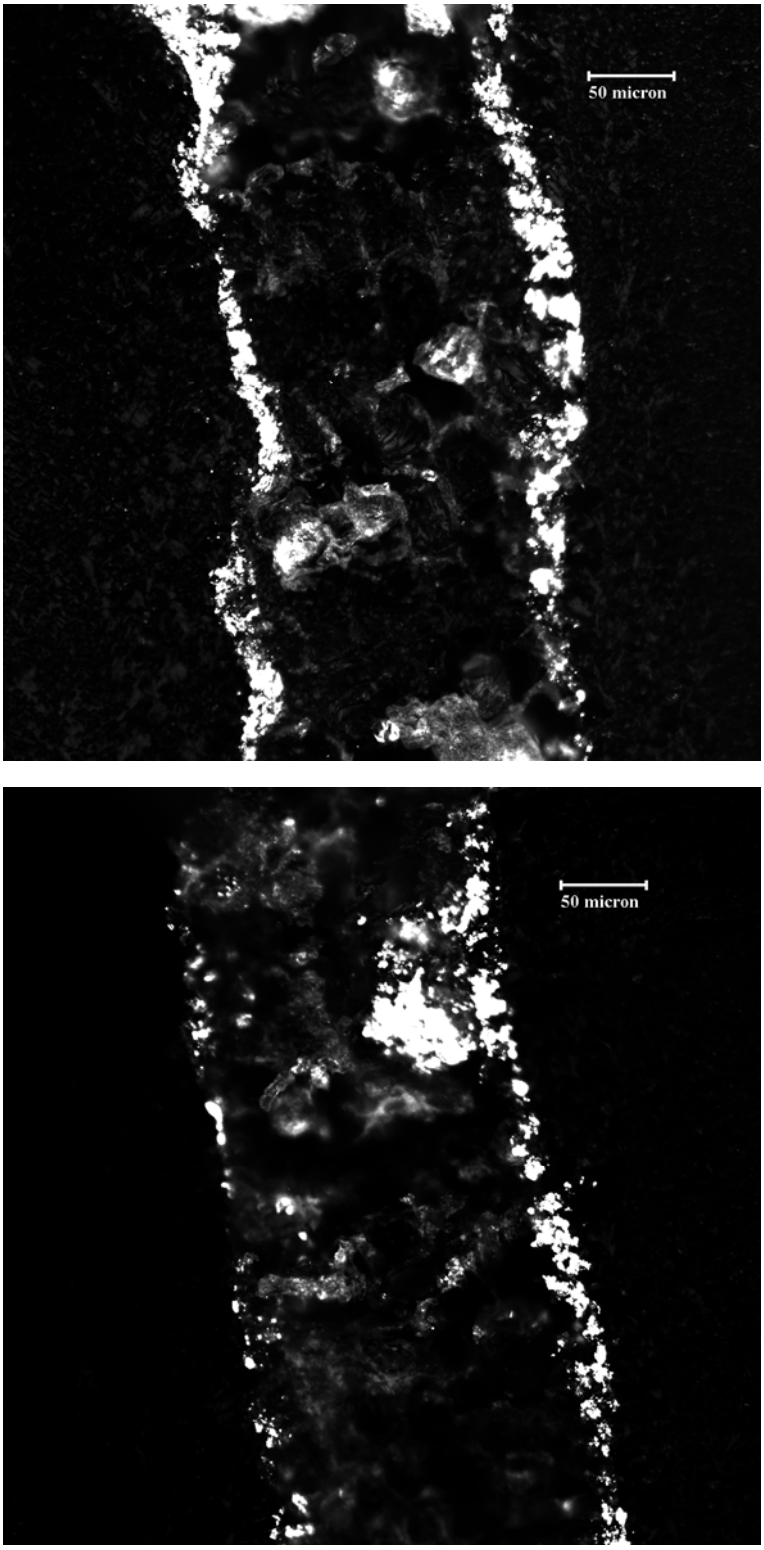

Figure 18: Shows two microscope pictures of a wooden piezoelectric sample. The bright spots indicate the silver paint and, hence, electric conductance. The wood matter is situated in between the bright lines. Both images were taken from the same sample. The top image shows a region with comparably good coverage of the surface. The bottom has poor coverage on the left surface, and a pocket (likely due to a crack) filled with silver paint. Images were taken with an Olympus BX51 microscope, using polarized light.

4.1.1.2. Regenerated Cellulose

In addition to the wood samples, samples of regenerated cellulose were produced with different ratios of crystalline/amorphous cellulose. The goal was to produce a material that would allow the investigation of the influence of the degree of crystallinity and was as well comparable to wood. The same objectives as mentioned in 4.1.1.1 had to be met. The shape had to be similar to the wooden samples.

To obtain samples with different crystallinity, the amount of the starting material (ground cellulose powder) was varied while keeping the other ingredients constant. The amount of solvents was adequate to dissolve 6 g of cellulose. If the amount of cellulose was raised, while keeping the other ingredients constant, the solvent could not dissolve all the cellulose. Hence, parts of it remained undissolved. Since these parts had a much higher crystallinity than the dissolved parts, this was an effective possibility to vary the degree of crystallinity of the different cellulose foils.

4.1.1.2.1. Production of the Cellulose Foil

The following steps were carried out to produce the desired samples.

- Start: the cellulose powder (6/8/10 g) was activated in tap water (200 ml) for one hour. Stirred after 30 min.
- 60 minutes: the cellulose sedimented to the bottom of the container. The water was cast and replaced with methanol (200 ml).
- 90 minutes: the cellulose sedimented and the methanol was replaced with another 200 ml of fresh methanol.
- 120 minutes: the methanol was replaced with acetone (200 ml)
- 150 minutes: the acetone was replaced with dimethylacetamide (200 ml). Simultaneously, a solution with 16 g lithium chloride and 200 ml dimethylacetamide was prepared (constant stirring for 60 min).
- 180 minutes: the dimethylacetamide was replaced with another 200 ml dimethylacetamide.
- 210 minutes: the dimethylacetamide was replaced with the lithium chloride solution. This dissolves the cellulose. As soon as the solution started to jell, it was poured into three rectangular glass bowls (20 x 30 cm). The fluid level was about 2 to 3 millimeters high.
- 24 hours: the solvent evaporated leaving cellulose-films behind. After filling the bowls with warm water the films detached from the bottom.

The water removed the remaining solvent. This was especially important since the resulting material needed to be nonconductive.

Figure 19: Cellulose films in various stages of drying. Left (6 g) is ready for further manipulation whereas the middle (8 g) are amidst the drying process and the right (10 g) foils are still wet.

- 26 hours: The cellulose-films were transferred to a larger container filled with tap water (5 liters). The water was replaced after another 2 hours.
- 48 hours: The films were now ready for drying.

Drying was carried out by placing the films in between standard printer paper. The paper was replaced five times during a 48 hour period. Afterwards the films were stiff and dry enough for further manipulation.

4.1.1.2.2. Stretching of the cellulose-foils

Due to the dissolving and precipitation process, all the cellulose including the crystalline regions were unoriented. But a macroscopic observable piezoelectric effect requires the crystals to be oriented. Hence, the cellulose foils needed to be stretched. This aligned any fibrous elements within the foil along the direction of the tension.

Prior to stretching, the foils were immersed in tap water for about 5 minutes. This resulted in considerable swelling and softening of the material. Subsequently 6 cm broad strips were cut from the foils. These were clamped in a universal testing machine with an initial gauge of 7 cm. The samples were first attempted to be stretched for an additional 3 cm (+43%). This stress could only

be bared by the 6 g foil. Subsequently the elongation was reduced to 2 cm (+30%), a displacement that was acceptable for all the foils.

Table 6: Elongation of the stretched foils. 6, 8 an 10 g are subject to the initial amount of ground cellulose used for producing the foils.

Material	Elongation
6 g Foil	30 mm, 43%
6 g Foil	20 mm, 29%
8 g Foil	20 mm, 29%
10 g Foil	20 mm, 29%

Figure 20: Cellulose-films before and after stretching. This sample is a cellulose-film with 6 g cellulose. The dotted line shows how the Piezo specimens were cut out of the dried and stretched foils. (Scale in centimeters)

As soon as the target length was obtained the specimens were blow-dried with hot air. Simultaneously the applied stress was observed. Due to the drying and consequently shrinkage the stress was increasing. The blow drying continued until the tensile stress leveled off which meant that most of the water had already evaporated. Thereafter the foils were flatted by a hot iron which also removed most of the remaining moisture.

4.1.1.2.3. Conductive Paint

From the stretched and dried cellulose foils piezo specimens were cut as shown in Figure 20. The samples' surfaces were then painted with conductive paint (Silber Leitlack 5900, Busch GmbH, Viernheim, Germany). Subsequently the edges were sanded to obviate any current flow between the surfaces. Thereafter the samples were stored in a desiccator to prevent any influence of the moisture content which would come to effect on an MC above 6% (Nakai, Igushi, & Ando, 1998).

4.1.2. Electrical Source

The electrical power for establishing the DC electric fields was provided by several transformers in a serial connection. Each transformer had a given voltage conversion rate, and, hence, only a few fixed output voltages were available. So, the amplitude of the electrical field was a discrete value. The turning on/off of the transformers required pressing of several buttons and took ~ 1 to 2 seconds. The maximum available DC voltage in the Vienna lab was 310 V, and was 248V for the experiments in Leoben[6].

4.1.3. Direct Stress Measurement

4.1.3.1. Principle of Measurement

The converse piezoelectric effect causes a deformation of crystalline materials induced by an electric field. To detect this deformation it was necessary to create an experimental setup that allowed measuring of the actual stress on the specimen while enabling the application of direct-current up to 310 volts. The specimens were coated with conductive paint along the surfaces. To avoid any possible current flow to the testing machine, an insulated clamping device was used.

Before the electric field was applied, an initial load was placed upon the specimens. Thereby they were perfectly oriented and any deformation caused by the converse piezoelectric effect would result in a clear signal at the load cell. Especially for the wooden samples it was crucial not to exceed the maximum bearable load. The 0° samples were initially loaded with 10 N/mm², the 45° samples with 0.5 N/mm² and the 90° samples with 0.25 N/mm².

The cellulose foils were able to bear higher loads mostly because there was no cutting of the specimens necessary (contrary to the wooden samples) and the

[6] As described in 4.1.4.

density of the void-free cellulose foil was higher. Therefore the 45° samples were initially loaded with 10 N/mm².

4.1.3.2. Equipment Used

The direct stress measurements were carried out at a Zwick/Roell universal testing machine 020. Two different load cells were used: a 2.5 kN load cell for determining the mechanical properties of the wood samples with 0° and 22.5° orientation. For the other orientations and all the piezoelectric experiments a 50 N load cell was sufficient.

4.1.3.3. Experimental Setup

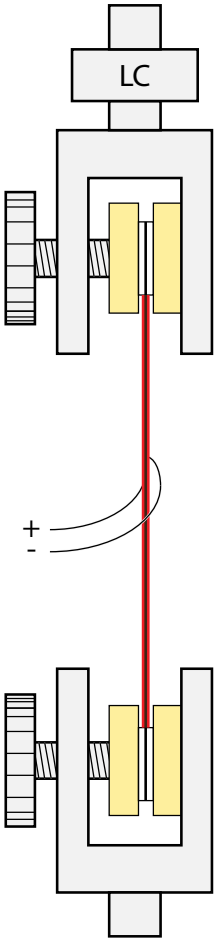

Figure 21: Schematic draft of the experimental setup used to detect the converse piezoelectric effect. The light yellow block demonstrates the insulating material in the clamps. The red lines indicate the conductive paint, applied on the surfaces of the specimens. LC stands for load cell.

The experimental setup for the direct stress measurements was basically a regular tensile test design. The samples were fixed and pulled along the longitudinal axis, a load cell measured the stress. The electric field was applied by tow wires that were affixed in a way that they did not perform any significant load to the specimens. Due to the application of an electrical field, the specimen

had to be insulated from the testing machine. This was guaranteed by polymer blocks attached to the clamps. Figure 21 illustrates the experimental setup.

Depending on the investigated material, different voltage and thickness resulted in a varying electric field. Table 7 gives an overview of the properties of the specimens and the applied voltage.

Table 7 shows materials used for detecting the converse piezoelectric effect by mechanic measurements.

Type of Material	Fibre Angle	Thickness [mm]	Voltage [V]	Electric Field [V/mm]
Cellulose Foil[7]	45°	0.2	310	1550
Wood (*Pinus sylvestris*)	0°	0.2	243	1215
Wood (*Pinus sylvestris*)	45°	1.8	310	172
		0.2	166	830
		0.2	84	420
		0.2	42	210
Wood (*Pinus sylvestris*)	90°	0.2	243	1215
PE-Foil (Placebo)	-	0.07	310	4430

4.1.4. Wide Angle X-ray Scattering Measurement

4.1.4.1. Principle of Measurement

The underlying hypothesis of this research work was that the application of an electric field on thin wood and cellulose samples will result in an observable macroscopic shift in shape. Furthermore this reaction is likely triggered by a converse piezoelectric effect. This piezoelectric effect (as described in chapter 3) results in a modification of the shape of a crystallite. To prove that the macroscopic reaction in wood and cellulose materials is caused by this phenomenon one has to find a method that could determine whether or not the cellulose crystallites change the shape when applying an electric field.

[7] Since the cellulose foils with the highest degree of crystallinity (produced with 10g cellulose powder) resulted in a hardly detectable piezoelectric response, the foils with 6 and 8 g cellulose powder were neglected in further testing.

This can be accomplished by the means of WAXS (wide angle x-ray scattering) which provides a possibility to acquire a 2D scattering pattern that depends on the specifications ($a, b, c, \alpha, \beta, \gamma$) of the crystallite's unit cell (Bower, 2002).

WAXS uses a highly focused monochromatic x-ray beam that impacts the analyzed material. If this material consists at least partly of crystals, this beam is reflected in a very specific way. Unlike a mirror where the beams are all reflected on the surface, the reflection of an x-ray beam in a crystallite follows Bragg's law (Figure 22).

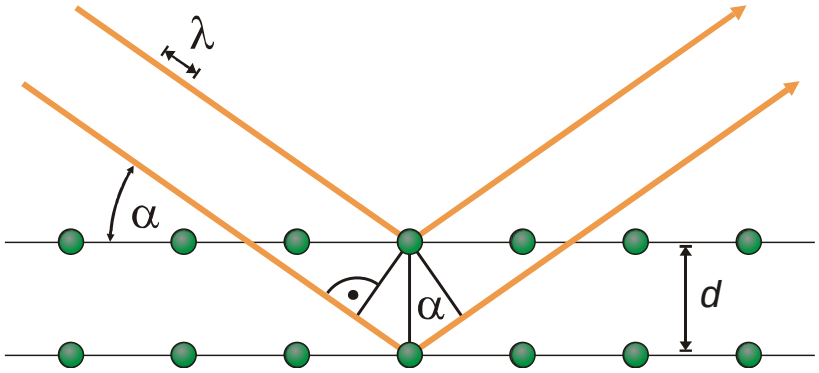

Figure 22: X-ray reflection in a crystallite according to Bragg's law. (Prior, 2009). α indicates the angle on which the radiation hits the surface, λ gives the wavelength of the x-rays. The beams can be assumed to be parallel due to the relatively far away radiation source.

The rays in the beam can be assumed to be quasi-parallel due to the relatively far away placed x-ray source. These rays have a very short wave-length (those used in polymer studies λ = 0.1-0.2 nm) and can be reflected at the crystallites layers (Bower, 2002). Bragg's law states that constructive interference of the waves can occur. This, however, requires a certain angle α that is determined by the wavelength λ and the distance d between the crystalline layers (Prior, 2009). The variable n (only natural numbers) connotes that the rays are reflected at several layers, n denoting the order of the layer.

$$2d \cdot \sin\alpha = n \cdot \lambda$$

This formula says that if the distance covered by the ray while traveling between the first and second (or n^{th}) layer is a multiple of the wavelength, the phases of the waves will constructively interfere when the ray comes back on the first layer. This can only happen at a certain angle. Hence, the crystallite reflects the monochromatic (but not polarized) beam according to the layers in its unit cell

(Bower, 2002). These reflections can be recognized by a detector. If the crystallites in the analyzed matter have a preferred orientation the recorded scattering pattern will possess regions with stronger intensity and regions with lesser intensity. If, according to the hypothesis, the crystallites shape is modified by an electric field, this modification will result in a different scattering pattern.

4.1.4.2. Equipment Used

The WAXS measurements were carried out at the Erich Schmied Insitut (Monatanuniversität Leoben) using a Bruker Nanostar (Bruker AXS) system connected to a rotating anode generator with a Cu target. The system was equipped with crossed Göbel mirrors, a pinhole system for primary collimation with a beam diameter of 100 µm, and a two dimensional wire detector (Hi-Star).

The diffraction images obtained by the Nanostar were analyzed with the Fit2D software version 12.077 (acknowledgement to AP Hammersley/ESRF). In order to recognize any changes in the cellulose crystallites' structure θ and 2θ[8] scans were carried out.

Figure 23: The device used for obtaining the 2D-WAXS x-ray diffraction patterns, a Bruker AXS Nanostar system. The radiation was produced with a rotating anode generator with a Cu target (not displayed). The samples were put in a vacuum chamber. Wires for applying the electrical field were put in a gas tight feed through. (Image from a Bruker presentation, (Bruker ASX, 2009))

4.1.4.3. Experimental Set-up

The WAXS specimens needed to be penetrated by the x-ray beam while simultaneously applying the electric field. Therefore the samples were clamped using polymer blocks to insulate the metal housing. The electricity was applied

[8] θ refers to data analysis that integrates the resulting 2D image tangentially, 2θ refers to integration radially.

by two wires put through a gastight feed through in the housing. The x-ray source was approximately 1.5 m away from the specimen. To prevent any interfering influence from the atmosphere, the air was removed and the experiments were carried out in vacuum (see Figure 24).

To obtain a clear scattering pattern, it is necessary to irradiate over a certain time. In the case of the piezoelectric specimens the duration was 900 s or 1800 s. During that time, the specimens were left unmodified. At first the patterns for samples without an electric field were obtained, and afterwards with an electric field.

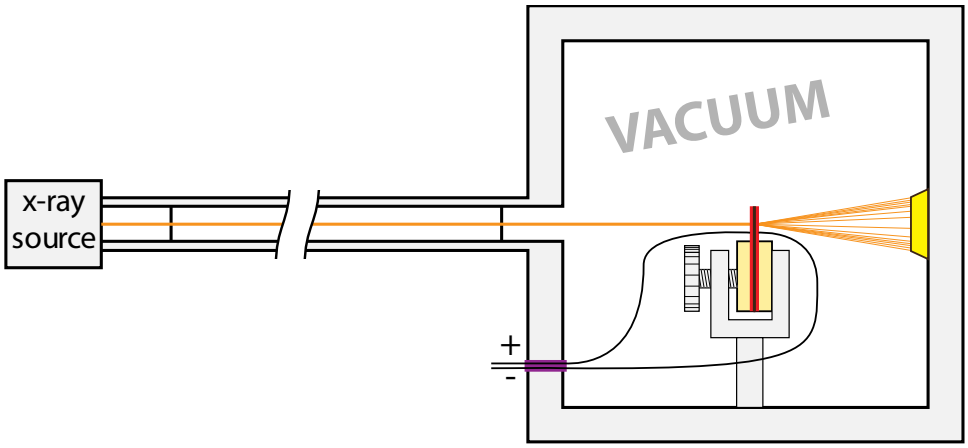

Figure 24: Shows a schematic draft of the WAXS experiments' setup (not true to scale). The sample is covered with conductive paint (red) and clamped with insulating polymer blocks (bright yellow). The x-ray source is about two meters away from the sample which allows obtaining a highly focused beam (orange). The reflection scattering pattern is collected by a two-dimensional detector (yellow).

4.2. Results and Discussion

4.2.1. Direct Stress measurement

The direct measurements recorded the stress applied to the specimens during the duration of the experiment. The gauge length was kept constant in that time. At first, the experiments specimens were pre-stretched, whereas the applied initial force depended on the strength of the samples, which was determined beforehand. This resulted in considerable relaxation during the test runs. The following charts show an example of the steps how to get a clear response curve from the original data.

Figure 25 shows the complete chart of one mechanic piezoelectric response experiment. This was the data as it was recorded from the load cell of the universal testing machine. In this example, the initial load was 0.5 N/mm². A

value, that decreased over time as is obvious. Hence, it was tried to subtract the relaxation function from the curve.

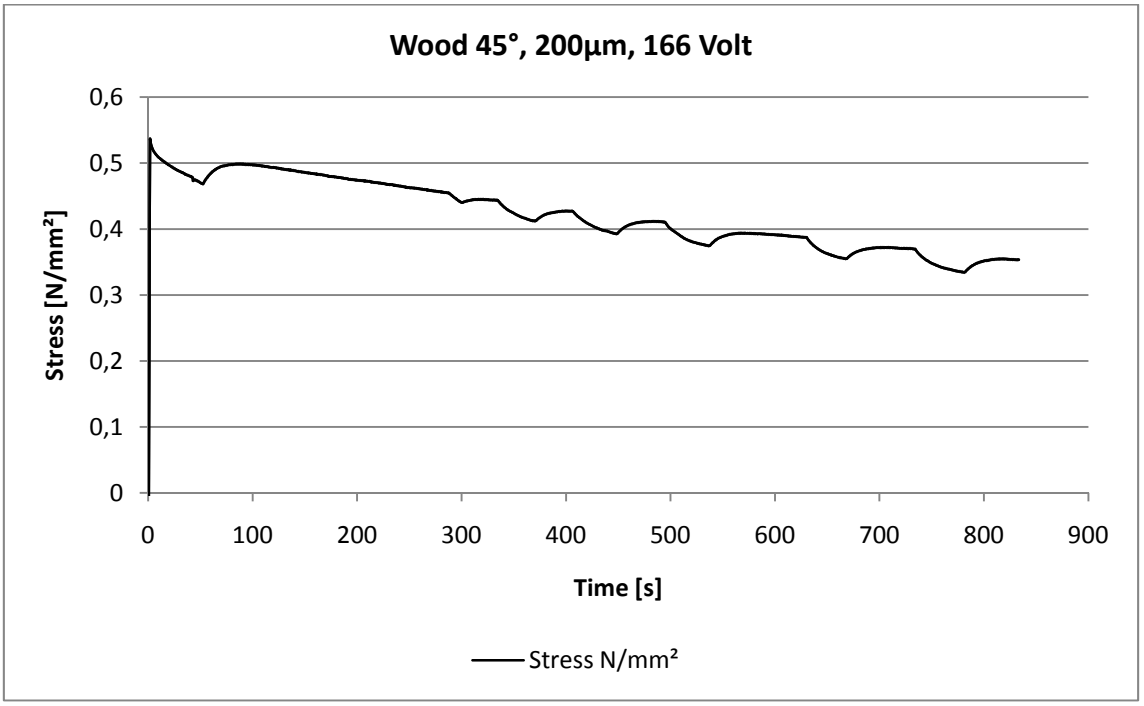

Figure 25: Complete chart of the piezoelectric measurement with a 45° fiber angle, 200 µm thick wood sample. The pre-load for the specimens before the application of the electric field was 0.5 N/mm². A certain trend caused by a relaxation of the sample is observable.

Therefore a certain region of the curve that showed clear signals was explicitly taken for calculating a trend line. In this example, it was the response measured in the time frame from 300 to 800 seconds. Using the “Add Trendline” function of Microsoft Excel 2007, an initial line was calculated.

This function, however, was often not satisfyingly reflecting the influence of creep. Hence, starting from the function that was provided by Excel, the trend line was adjusted by influencing the parameters. It should be noted, that depending on which time frame was used to calculate the trend line, different kind of functions were necessary to obtain good results. After all, following functions were used: exponential, logarithmic, polynomic (2nd order), polynomic (4th order).

At the shown example in Figure 26, an exponential trend line function ($y = 0.517 \cdot e^{-x \cdot 0.000457}$) was satisfyingly presenting the relaxation’s influence.

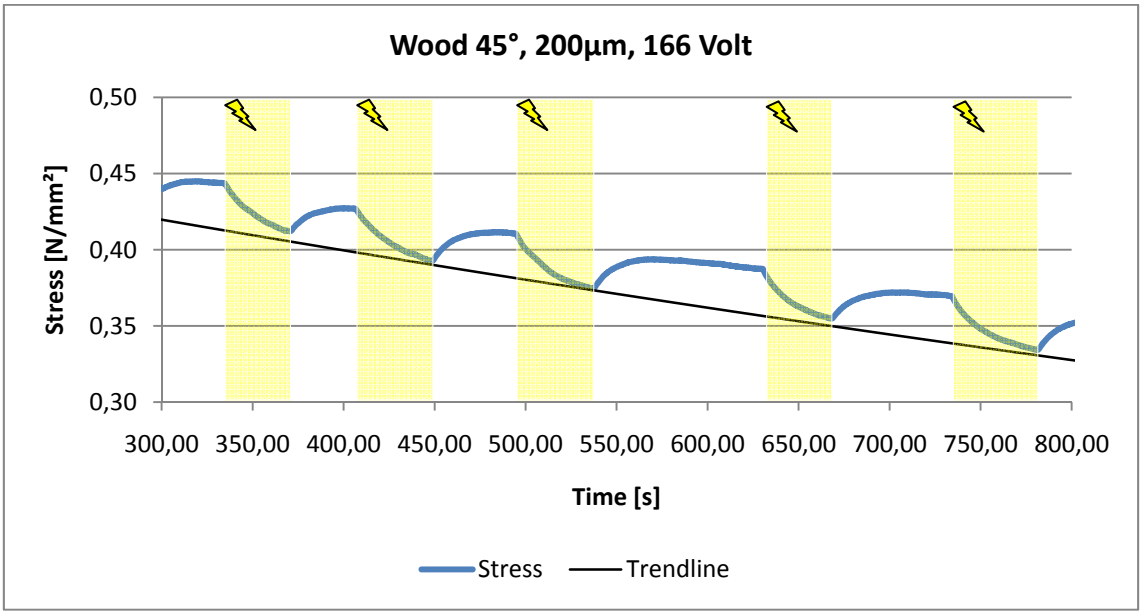

Figure 26: Shows a magnification of the region in Figure 25 where the electrical field was applied. The yellow marked periods define the time with a present electrical field of 830 V/mm. The specimen was 0.2 mm thick pine wood with a fiber angle of 45°. The shape of the reaction curve is most likely caused by the characteristic capacitor line which shows very similar gradient. Additional to the stress line a trend line was fitted to adjust to the relaxation of the specimen in the testing machine. The function of the trend line is $y = 0.517 \cdot e^{-x \cdot 0.000457}$

Once this influence was subtracted from the response curve, the resulting curve was showing the pure piezoelectric effect and is therefore comparable. Figure 27 shows such an exemplary curve.

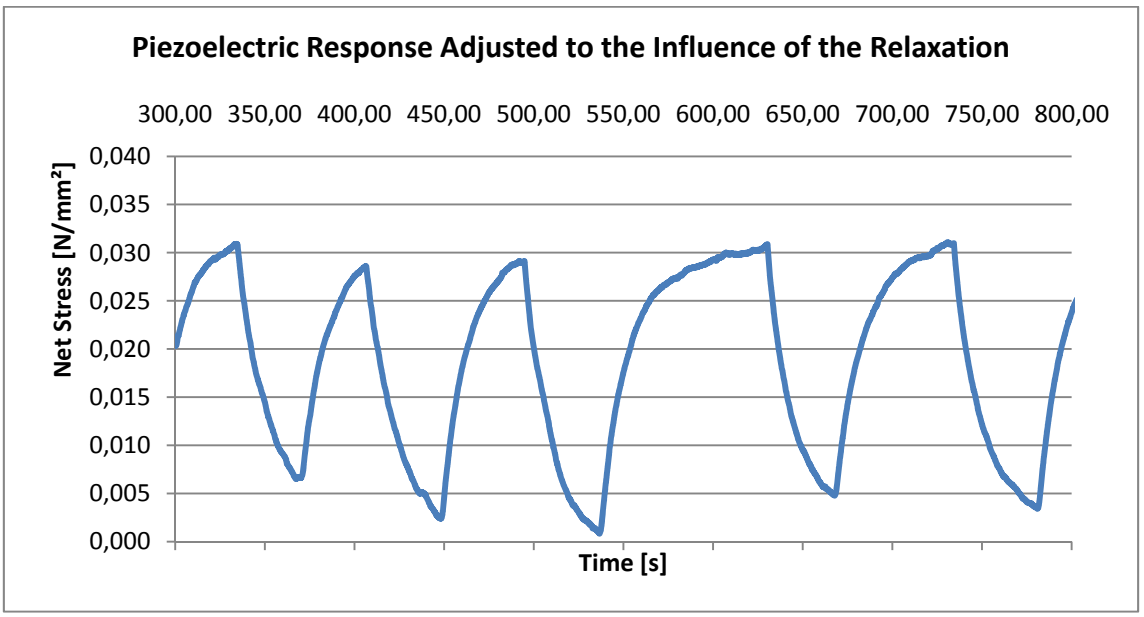

Figure 27 shows the piezoelectric response adjusted to the relaxation curve demonstrated in Figure 26. Without the influence of relaxation, the extent of the piezoelectric effect is clearly visible, amounting about 0.03 N/mm².

4.2.2. Direct Measurements Wood

4.2.2.1. Thin wood sample

With the thin wood sample, thickness of 200 µm, and a fiber orientation of 45°, very good measurements could be taken. A 45° fiber orientation was chosen since all available literature indicates a shear piezoelectric effect. Hence, the mechanic response would be greatest with a 45° orientation.

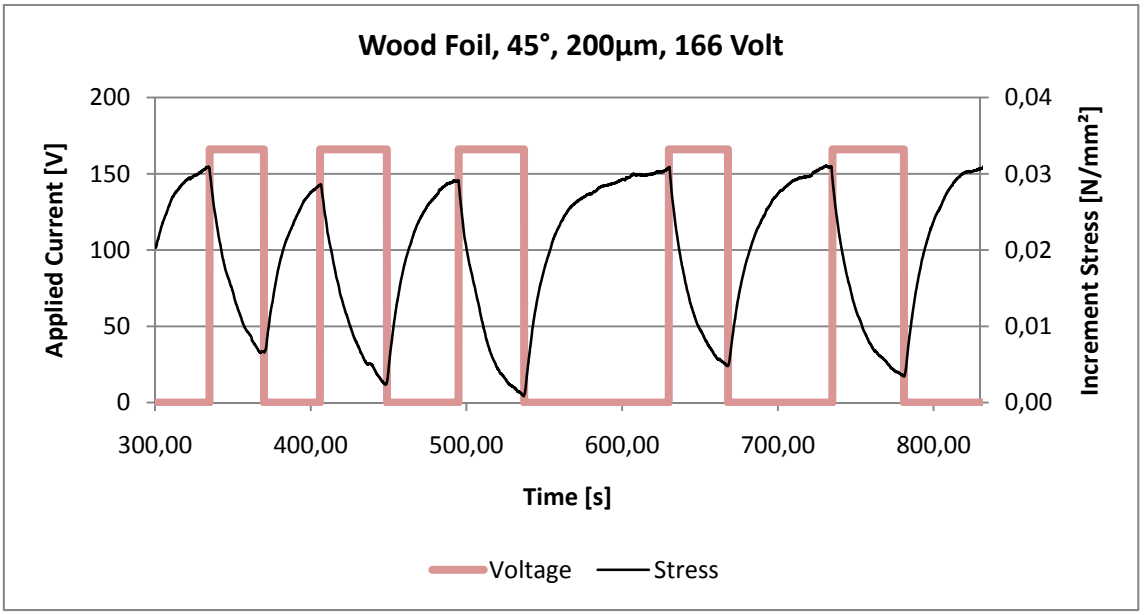

Figure 28: Piezoelectric response of a thin wood sample. Thickness 200µm; applied voltage 166 V; fiber orientation 45°; initial load 1 N/mm²; relaxation adjustment function: $y = 0.517 \cdot e^{-4.57 \cdot 10^{-4} x} - 0.031$

The applied current was initially 310 V. In that case, though, a short-circuit appeared and, hence, the voltage was reduced to 166 V. This sample showed a very strong piezoelectric response, clearly assignable to the electric field. The response curve is illustrated in Figure 28. The black line shows the stress (adjusted to creeping), the red line indicates the applied current. This voltage, though, is an assumption since the switching-on as well as the charging of the capacitors takes some time as explained in 4.1.2.

For a basic understanding of the relationship between the amplitude of the electric field and the amplitude of the mechanic response, the voltage was reduced by 50% for two consecutive runs. Figure 29 and Figure 30 show the according data. The scales of the axis are the same as in the initial experiment, for better comparability.

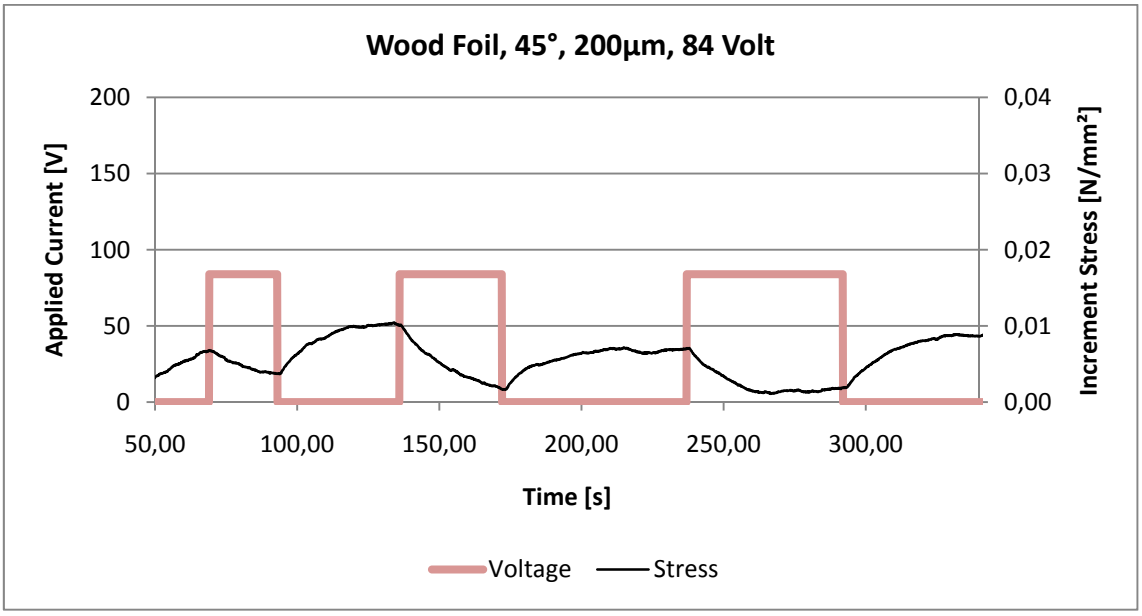

Figure 29: Piezoelectric response of a thin wood sample. Thickness 200µm; applied voltage 84 V; fiber orientation 45°; initial load 1 N/mm²; relaxation adjustment function: $y = 2.24 \cdot 10^{-11}x^4 - 2.09 \cdot 10^{-8}x^3 + 7 \cdot 10^{-6}x^2 - 1.16 \cdot 10^{-3}x + 0.525$

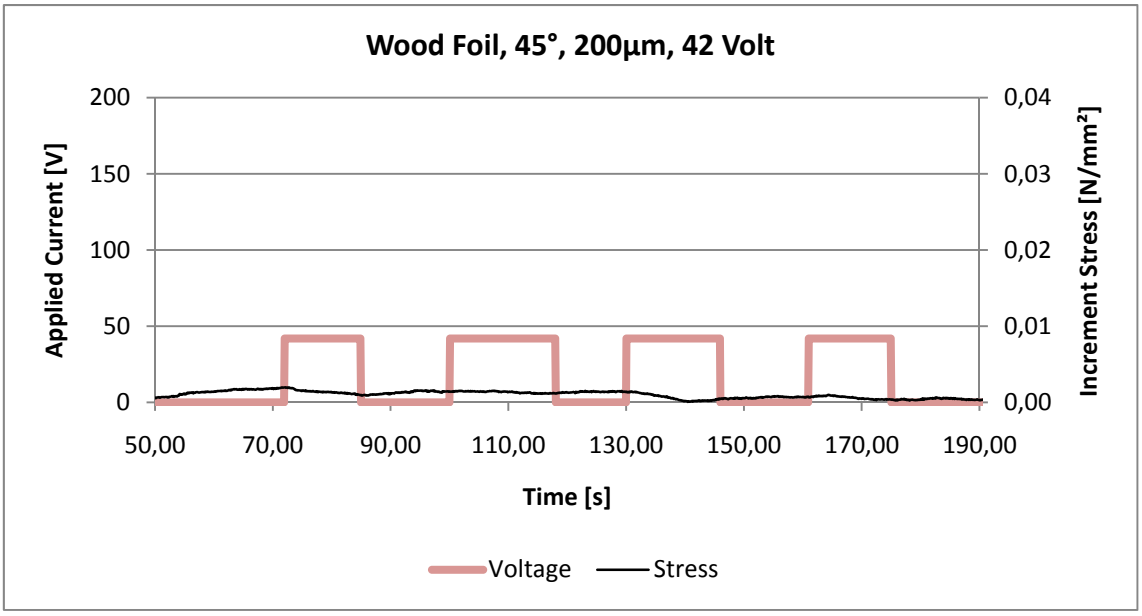

Figure 30: Piezoelectric response of a thin wood sample. Thickness 200µm; applied voltage 42 V; fiber orientation 45°; initial load 1 N/mm²; relaxation adjustment function: $y = 6 \cdot 10^{-11}x^4 - 3.3 \cdot 10^{-8}x^3 + 7 \cdot 10^{-6}x^2 - 8.4 \cdot 10^{-4}x + 0.5178$

Figure 31 shows a chart of the relationship between amplitude of the mechanic response and the applied current. Obviously, the mechanic response is a non-linear relationship against the applied voltage. An exponential function has been fitted to illustrate a possible non-linear behavior. Still, this can only be seen as indication, since the three data points (166, 84, and 42 V) are not suitable to

give a significant conclusion. Further research in this interrelation between the amplitude of the electric field and the mechanic response is necessary.

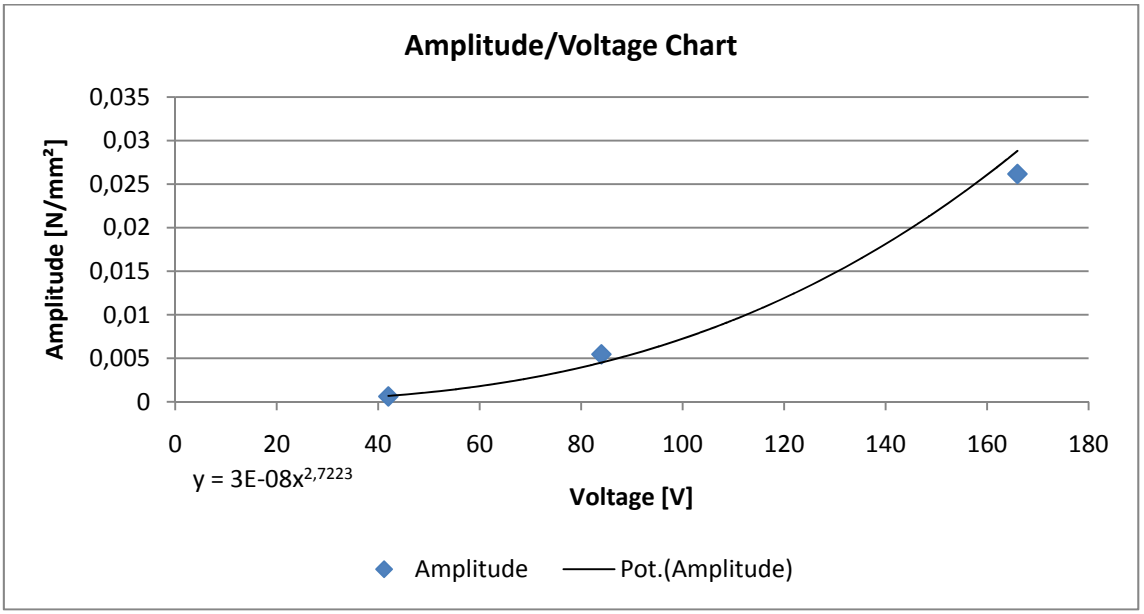

Figure 31: Amplitude of the mechanic response vs. the applied voltage of the experiments shown in Figure 29-31. The difference between the maximum and minimum stress within one on/off electrical field cycle was calculated and plotted against the applied voltage. A trend line indicates a non-linear behavior relationship between the variables, but three data points (four data points, assuming that at the trend line has to pass the origin 0/0) are not suitable for any significant conclusion.

4.2.2.2. Thick wood sample

The thick wood samples had a thickness of 1.8 mm[9]. Unlike the thin wood samples, a clear piezoelectric signal was not acquirable. Figure 32 shows a chart of the adjusted response curve. The scale of the differential stress is 10^2 times smaller compared to the thin wood samples. Still, the response curve does not seem to be influenced by an electric field.

The missing piezoelectric response might be explained by the lower extent of the electric field (172 V/mm, s. Table 7) compared to thinner wood samples. Nonetheless, the thin wood sample shown in Figure 30 was exposed to an electric field of 210 V/mm, not much higher. The actual reason for this non-response is still unknown. Further research of the piezoelectric properties of wood in respect to its dimensions and orientation might be helpful for a deeper understanding of the observed occurrences.

[9] This thick wood sample is one of the samples used for mechanical characterization as described in chapter 4.1.1.1.3. Due to sanding for a perfectly uniform cross-section, the thickness was reduced from 2 mm to 1.8 mm.

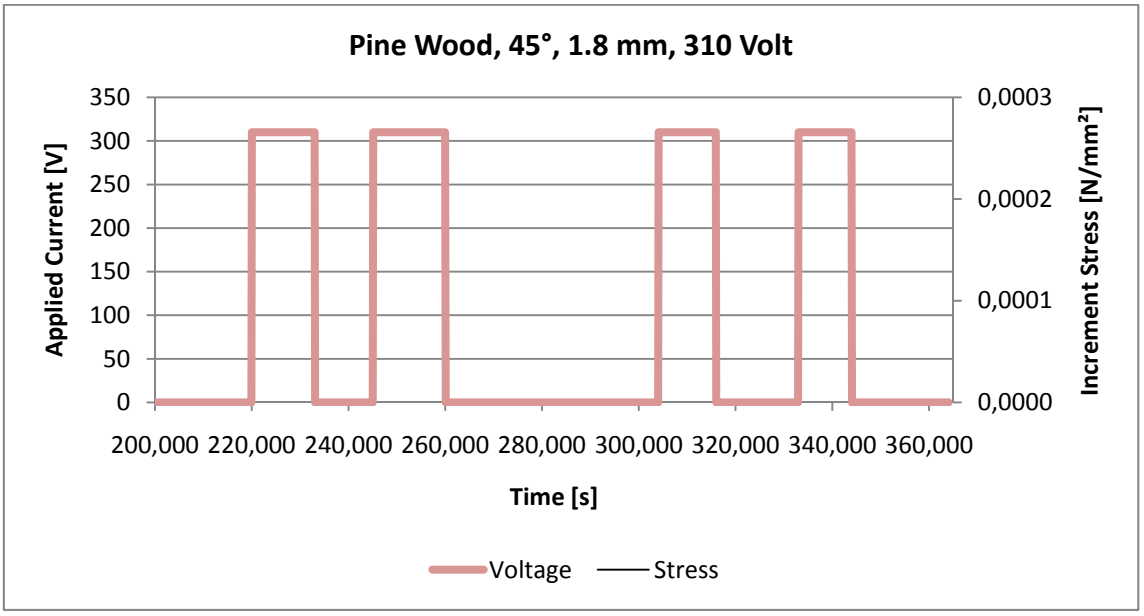

Figure 32: Piezoelectric response of a thick wood sample. Thickness 1.8 mm; applied voltage 310 V; fiber orientation 45°; initial load 1 N/mm²; relaxation adjustment function: $y = -9.99 \cdot 10^{-13}x^4 + 1.11 \cdot 10^{-9}x^3 - 3.8 \cdot 10^{-7}x^2 - 7.2 \cdot 10^{-6}x + 0.971$

4.2.2.3. Comparison of different fiber orientations

After the initial piezoelectric experiments showed a distinct piezoelectric effect for wood, the dependence of its amplitude in respect to the fiber angle was investigated. Therefore, three samples (s. 4.1.1.1.2) from the same piece of a wooden sheet were exposed to an electric field.

Figure 33 shows the surprising results. In this chart, the differential piezoelectric response (adjusted to relaxation) is shown for the three different fiber angles. According to the literature (e.g. (Fukada, 1955) or (Bazhenov, 1961)), the direct piezoelectric effect in wood is causing shear deformation. This is still the common theory. According to that assumption, one would expect the biggest deformation caused by the converse piezoelectric effect of the samples in a 45° fiber angle.

The results however, showed a clearly higher response in the 90° fiber angle. Although the chart is a little bit misleading since the voltage was not equal for every sample, the explicitly larger response by the 90° sample compared to the 45° sample cannot solely be explained by a stronger electrical field.

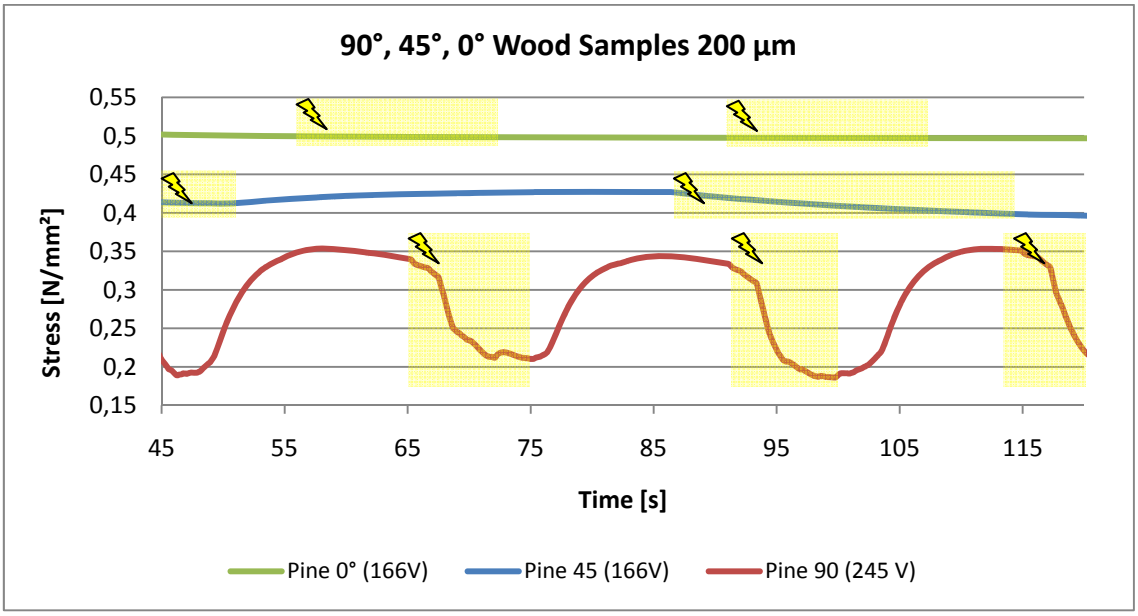

Figure 33: Comparison of the piezoelectric response with respect of the fiber angle. The wood samples were cut from the same piece of a 200 µm thin sheet of wood. The 90° sample was exposed to 245 V DC, the 45° and 0° samples were exposed to 166 V.

4.2.3. Direct Measurements Cellulose

4.2.3.1. Cellulose Foils 45°

Since the research work was based on the assumption of a shear piezoelectric effect in wood, most of the cellulose samples were tested with a 45° angle. The response of the cellulose samples, though, was not as clear as those of wood.

The first sample with an evident response is shown in Figure 34. Although it was difficult to subtract the influence of relaxation in this curve, it is obvious that at the first four cycles the stress of the sample rises immediately after erecting the electric field. This is interesting since it was the first time that a rising stress was measured after exposure to the electric field, whereas the wooden samples always decreased in stress (i.e. lengthened a little bit) when exposed to the electric field. The second interesting occurrence was observable when the polarization of the applied voltage was changed. After that, the piezoelectric response seemed to have changed in polarization, too, resulting in a lower stress. Yet, this observation could not be repeated.

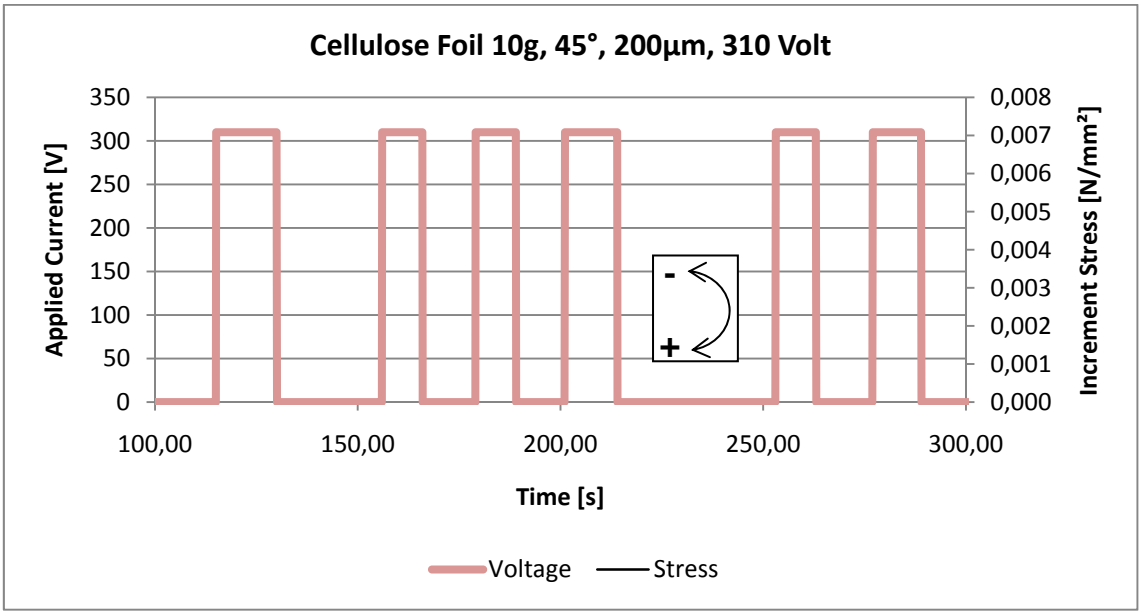

Figure 34: Piezoelectric response of a cellulose foil. Thickness 200µm; applied voltage 310 V; fiber orientation 45°. Reversion of polarity after the fourth turn. Initial load 10 N/mm²; relaxation adjustment function: $y = 8.6 \cdot 10^{-11}x^4 - 6.8 \cdot 10^{-8}x^3 + 2.08 \cdot 10^{-5}x^2 - 3.52 \cdot 10^{-3}x + 9.996$

Another, thinner, cellulose foil (Figure 35) exposed a much more distinct piezoelectric response. The first three peaks showed a response that looks fairly similar to the wooden response curves. But, again, after changing the polarization, the shape of the piezoelectric response clearly changed. Although it still resulted in a lengthening of the sample, the very first reaction was a short, but detectible, contraction.

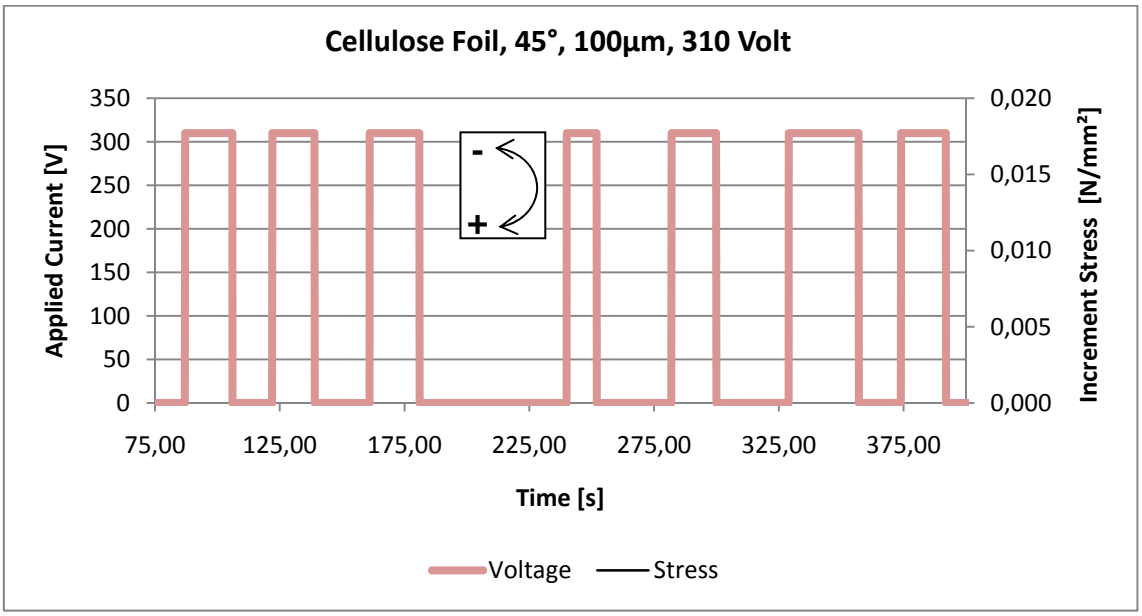

Figure 35: Piezoelectric response of a cellulose Foil. Thickness 100µm; applied voltage 310 V; fiber orientation 45°. Reversion of polarity after the third turn. Initial load 10 N/mm²; relaxation adjustment function: $y = 4.6 \cdot 10^{-11}x^4 - 5 \cdot 10^{-8}x^3 + 2 \cdot 10^{-5}x^2 - 4.57 \cdot 10^{-3}x + 9.913$

4.2.3.2. Influence of Different Fiber Orientations

For the cellulose samples the influence of different fiber orientation was investigated, too. Therefore, from the same stretched cellulose foil as shown in Figure 20, three samples with the orientation 0°, 45° and 90° were cut, covered with silver paint and subsequently analyzed. The influence of the fiber angle in cellulose samples seemed to be different than wood samples. The latter had a distinctively growing piezoelectric response in the order 0°-45°-90°; the cellulose samples didn't have such clear results. As shown in Figure 36, the 0° and the 45° sample had almost the same piezoelectric response amplitude. The 90° sample did not show a significant reaction at all.

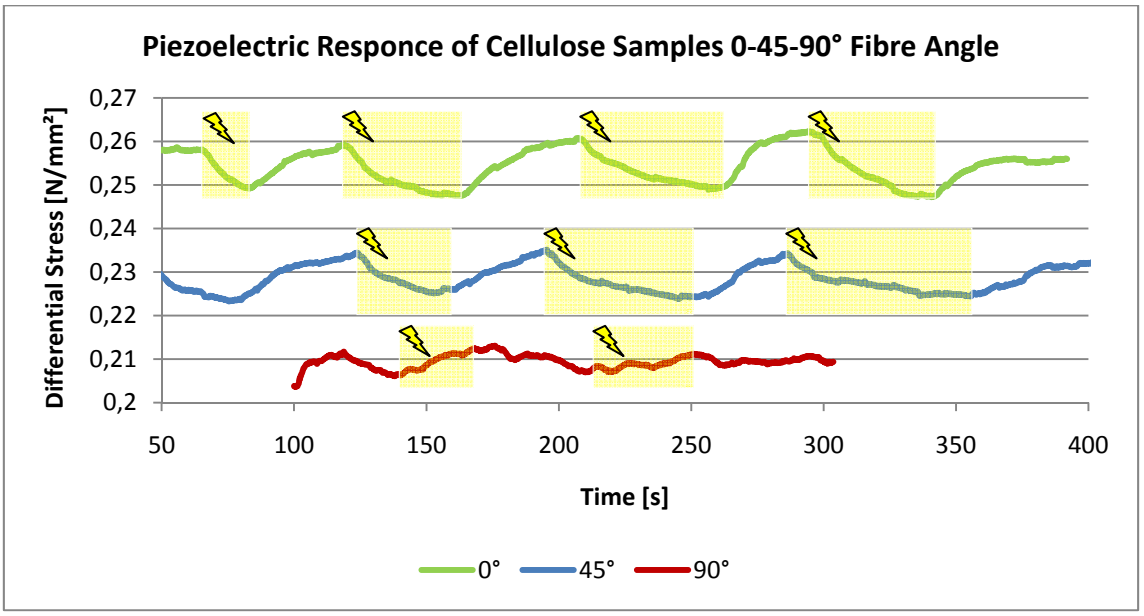

Figure 36 shows the mechanical response of the cellulose foil. The three lines indicated different fiber orientation (0, 45 and 90°). The regions defined by the arrows indicate an applied electric field. All response curves have been adjusted to creeping and for easier comparison put into one diagram whereas the y-axis goes without a unit.

4.2.4. WAXS-Measurements

Two-dimensional wide angle x-ray scattering measurements are a means of imaging and analyzing the characteristics of a material's crystallites. From the resulting images, diffractiograms can be generated. Therefore, the intensity of the radiation (the higher the intensity, the darker the spots) is integrated along a proper axis.

The initial assumption was that the piezoelectric effect in wood is of a shear type. A logic deduction is that one would expect a shift in the cellulose unit cell's orientation. This could be verified by integrating along a centered circle from 0° to 360°. With a shift in orientation, the dark spots on the image and therefore

the peaks in the diffractiogram would alter their position. Nevertheless, comparing such a centered diffractiogram of 0V with 166V didn't show any differences. Therefore, another integration axis (the 2θ-axis) was chosen. This diffractiogram shows the intensity of peaks along the Bragg angle. Figure 37 illustrates how those charts were calculated from the WAXS-image.

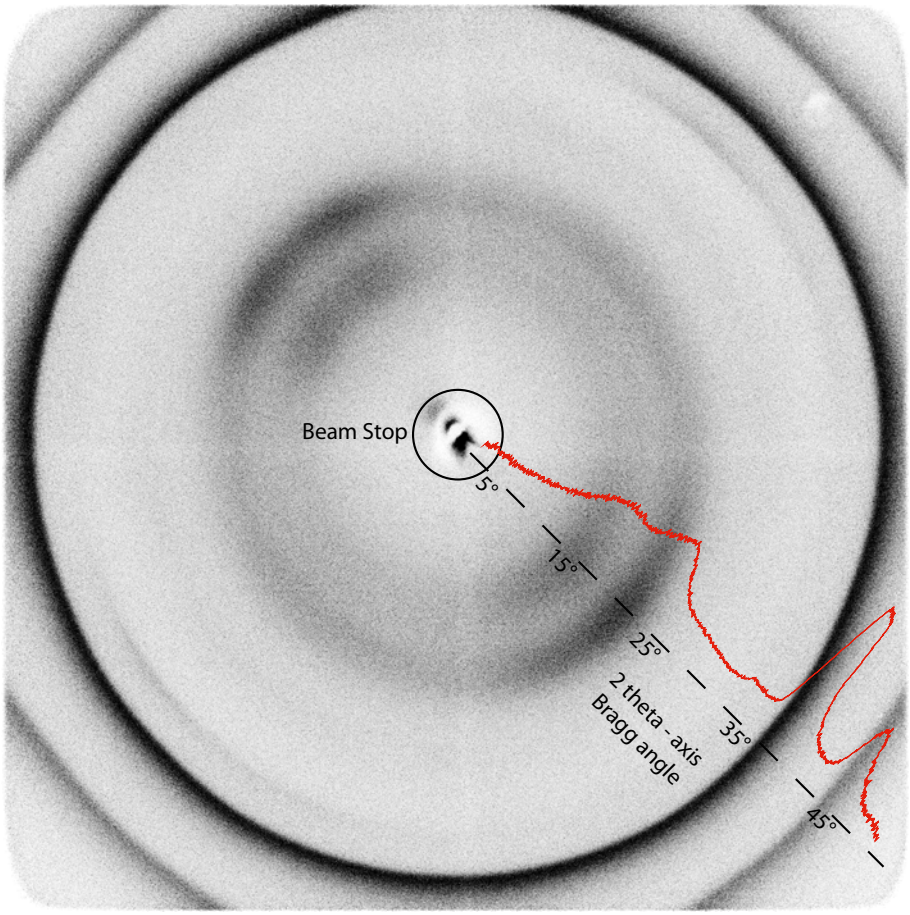

Figure 37: An x-ray diffraction pattern from a 200 µm wood specimen covered with conductive paint (containing silver). The dark outer ring shows the reflection from silver crystals whereas the inner, face-to-face positioned regions indicate a certain crystal orientation and shows the cellulose crystallites. For further analysis, the picture is integrated along the 2 theta axis. The result of the integration is shown by the red line; the 2-theta axis is marked by the dotted line[10].

These diffractiograms where obtained for wood and cellulose with various voltages and exposure times. Diffractiograms of the same material and exposure times were subsequently compared. Like in the direct stress measurements, there was a clear difference in the reaction between wood

[10] The value of the y-coordinate (here denoted as intensity) depends on the exposure time as well as on the image editing prior to integration. Therefore, the amplitude of the curve/peaks is only comparable to a limited extent.

(Figure 38) and cellulose materials (Figure 39). In total, three test series were carried out. The specifications are given in Table 8.

Table 8: Specifications of the WAXS measurements

Test run	Material	Voltage [V]	Exposure Time
1	Wood, 200 µm	0, 166	900
2	Cellulose 200 µm	0,166	900
3	Wood 200 µm	0, 166, 300	1800

At first, test run 1 and 2 shall be compared to illustrate basic differences in the response of wood and cellulose materials.

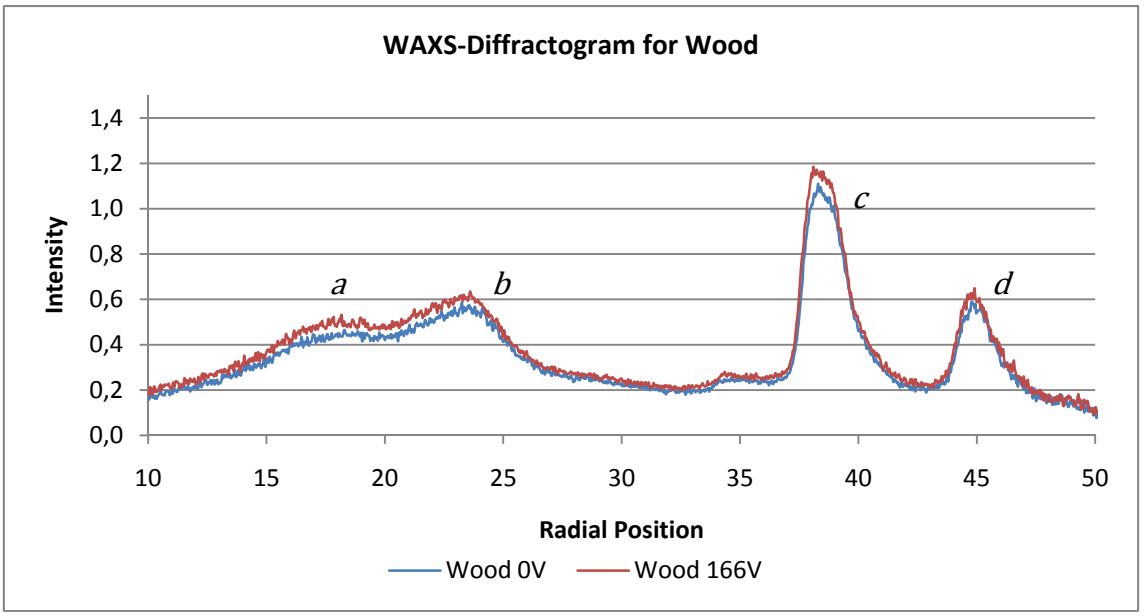

Figure 38: WAXS diffractiograms for wood (200 µm thickness). Exposure time was 900 seconds. The chart shows two measurements. The blue curve shows the response without an applied electric field, the red line shows the response under an electric field of 830 V/mm ($166\ V / 0.2\ mm$). a and b reflect the characteristic cellulose peaks, c and d are peaks from silver origin.

The two response lines obtained from wood with and without an exposure to an electric field were obviously non-congruent, hence indicating piezoelectric activity. The diffractiograms for cellulose with/without exposure to an electric field were almost exactly congruent. The very small meanderings can be explained by measuring errors. Hence, a shift in the cellulose crystallite's properties by a piezoelectric effect could not be detected by the applied WAXS measurements.

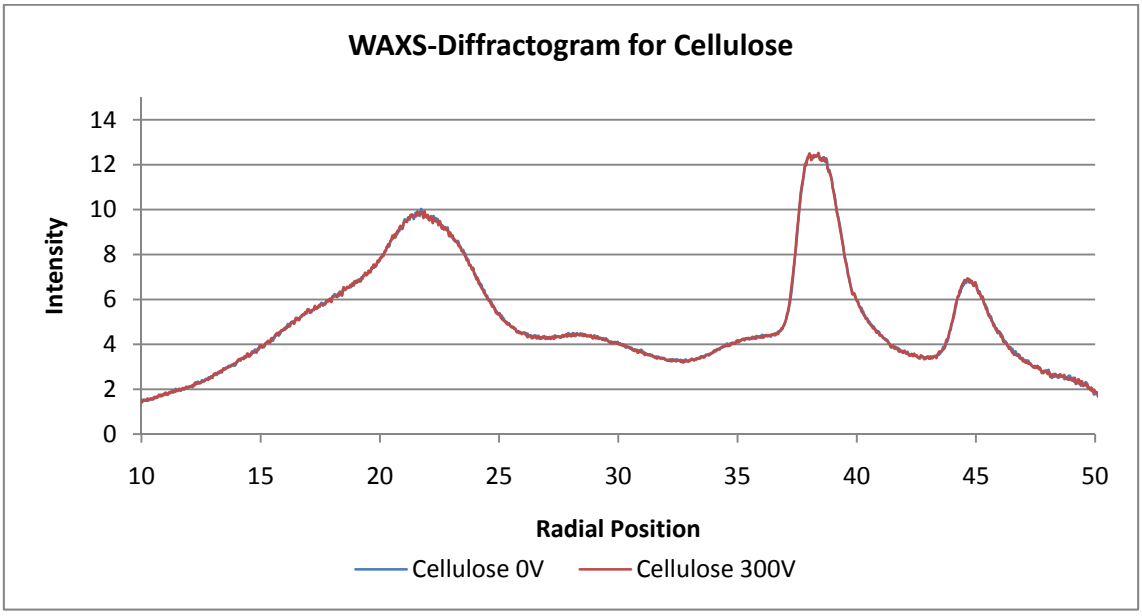

Figure 39: WAXS diffractiograms for cellulose (200 µm thickness). Exposure time was 900 seconds. The chart shows two measurements. The blue curve shows the response without an applied electric field, the red line shows the response under an electric field of 830 V/mm (*166 V / 0.2 mm*). The response does not indicate any shift in the crystal's properties under an electric field, since the two lines are congruent.

Starting from shown data, the radial position of the peaks was calculated. Using the *Fit Curve* function of the math software *Sigma Plot* (Systat Software Inc., Version 9.0) a *Gaussian 3-Parameter* curve was fitted into the peaks. The data range that was used for fitting den curves and the miller indices of the crystal layers of the according cellulose peaks *a, b* (Wada, Sugiyama, & Okano, 1993) are given in Table 9. Figure 40 and Figure 41 show the comparison of wood samples of run 1 and run 3 according to Table 9.

Table 9: The bragg angle range used for fitting the curves of the peaks. For the cellulose peaks (a, b), the miller indices for the according crystalline layers are given.

Peak	Bragg Angle	Miller Indices
a	15.23 - 19.73	(110)
b	20.42 - 25.61	(012) (120)
c	37.01 - 40.48	
d	42.9 - 46.39	

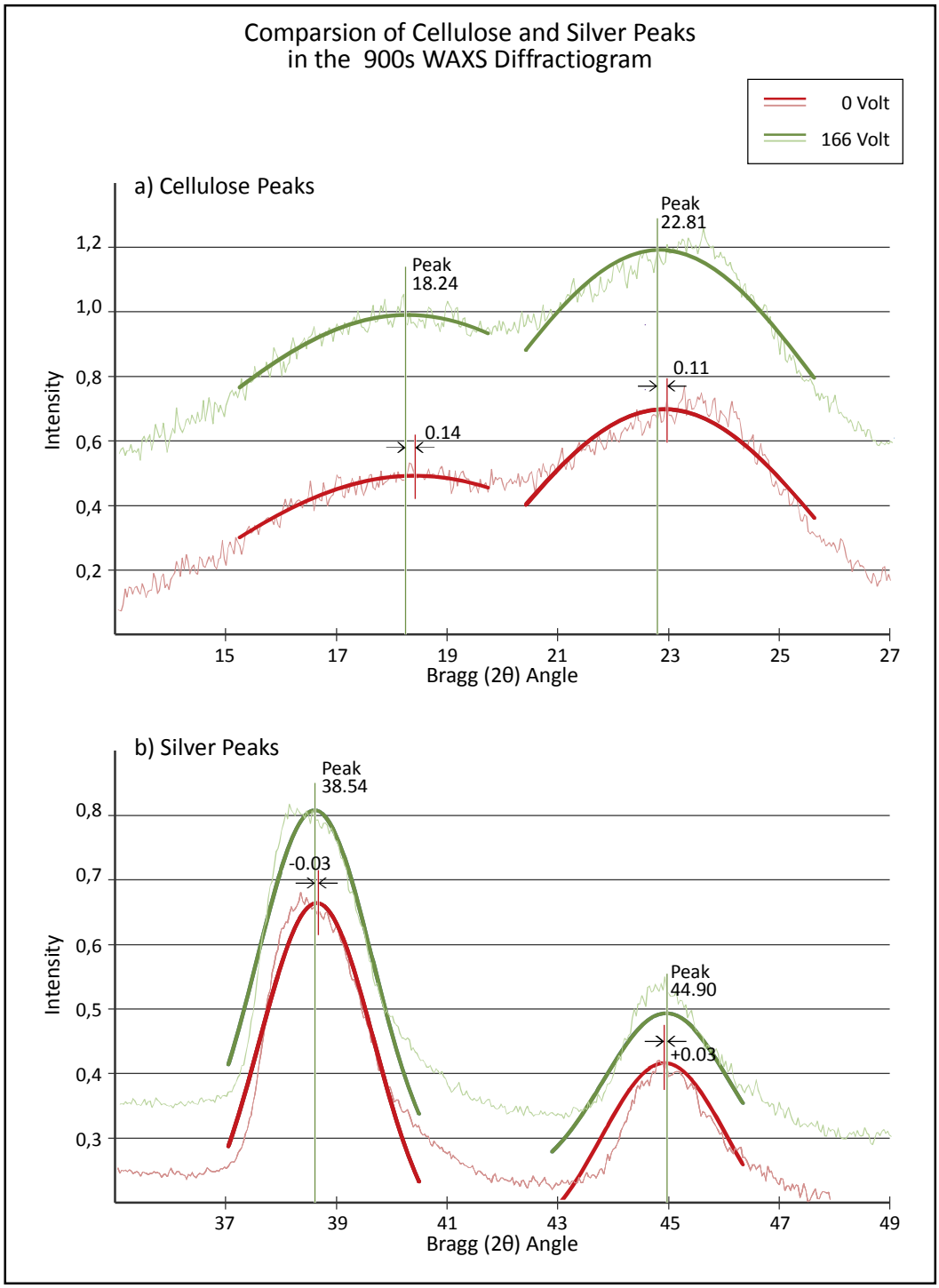

Figure 40: Comparison of wood sample (with/without exposure to an electric field) diffractiograms obtained by the means of WAXS (exposure time was 900s). The upper charts shows the peaks which are characteristic for cellulose, the bottom charts show the peaks of the silver paint. The solid lines show Gaussian curves, fitted in the peaks. For a better comparability, the lines have been offset.

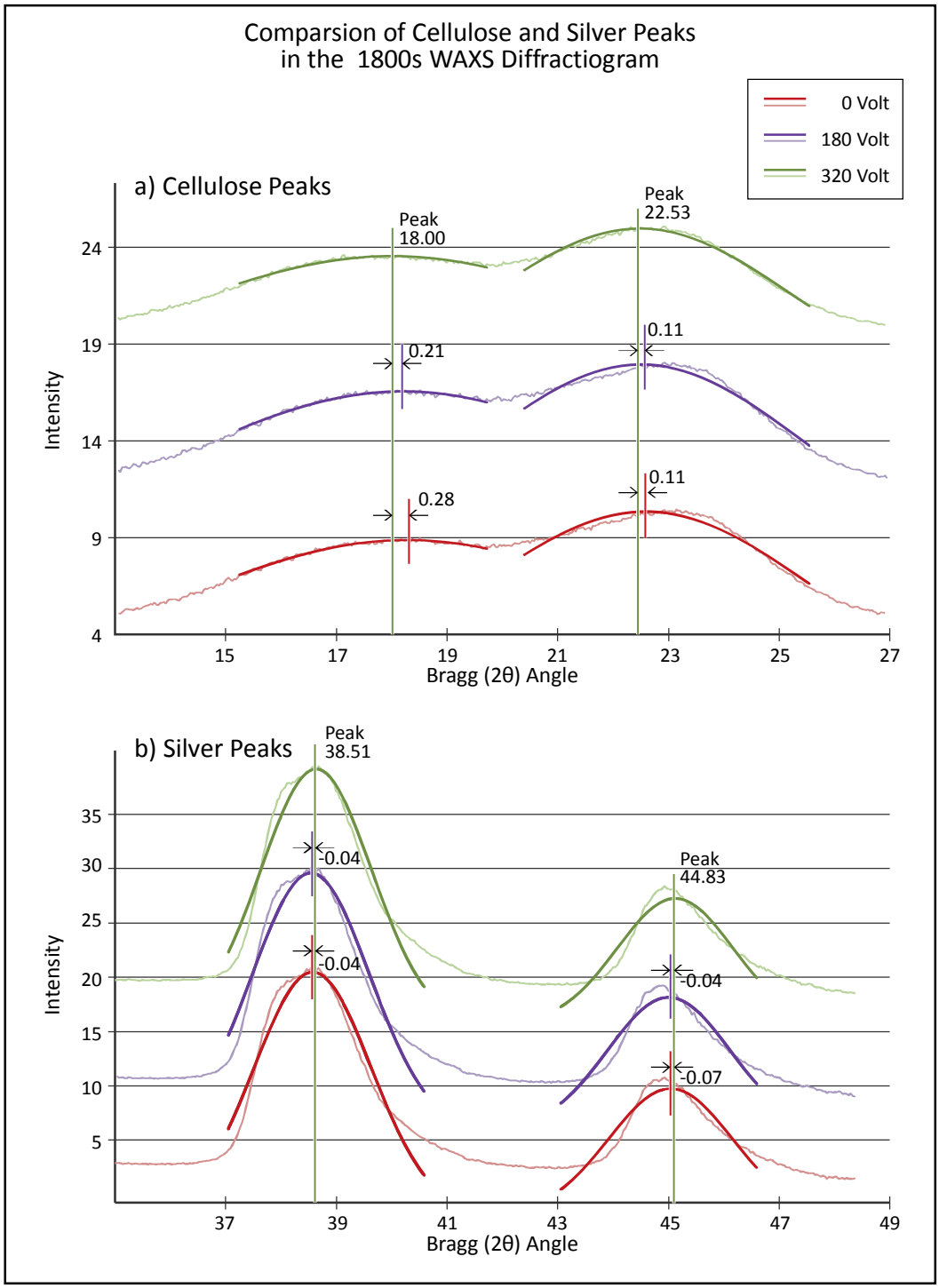

Figure 41: Comparison of wood sample (with three differently strong electrical fields voltage of 0/166/300 Volt) diffractiograms obtained by the means of WAXS (exposure time was 1800s). The upper charts shows the peaks which are characteristic for cellulose, the bottom charts show the peaks of the silver paint. The solid lines show Gaussian curves, fitted in the peaks. For better comparability, the lines have been offset.

In both charts, the shift of the fitted curves is distinctively bigger for the cellulose peaks compared to the shift of the silver peaks. Compared to the sample without exposure to an electric field, the samples under an electrical current all showed an offset towards a smaller Bragg angle.

5. Conclusion

5.1. Mechanical Measurements

The measurement of the converse piezoelectric effect provided interesting results. Despite a lack of statistical significance (due to the complex sample production and setup of the experiments most tests were carried out with only one specimen) following conclusions can be drawn:

Wood samples

- Small wood samples clearly react on an exposure of an electric field with elongation.
- The results indicate that the strongest reaction occurs in a 90° angle to the grain. For a 45° grain angle the piezoelectric effect is weaker and for a 0° grain angle, the effect is hardly detectable. This indicates that for the cellulose I crystallite, which is present in wood, it is not a shear-piezoelectric effect, but an effect perpendicular to the grain.
- The effect seems to grow non-linearly in respect to the amplitude of the electric field.
- Changing the polarity of the applied electric field did not have an influence on the shape of the reaction curve.

Cellulose-foils samples

- The effect in the cellulose samples is much smaller than for wood. Since the actual amount of the piezoelectric textures in wood (only cellulose I) and the cellulose foils (cellulose I and cellulose II) is not exactly known, this influence cannot be quantified.
- Due to the hardly measurable reaction on an electric field, no conclusions on the influence of the grain angle can be drawn.
- The change of polarity of the electric field resulted in a differently shaped reaction curve.

5.2. WAXS Measurements

The WAXS measurements supported and broadened the findings of the mechanical experiments. Since this method directly shows effects in the crystallite structures themselves, the expressiveness in terms of unveiling a piezoelectric effect in wood is very high. However, the result that certain peaks in a diffractiogram shifted (only in wood), needs to be further explained. As shown in Figure 40 Figure 41, the cellulose peaks a and b shifted left (along the

2θ-axis) whereas the silver peaks remained almost stable[11]. The shift to a lower Bragg angle indicates a widening of the cellulose molecules within the crystallite, or the unit cell respectively.

At least for the (110) (012) and (120) layers in the unit cell (Figure 42) a widening could've been shown. This is a clear indication that the crystallites and therefore the microfibrils widen which results in an elongation mainly perpendicular to the grain. The lattices II (012) and III (120) are indicated by the same peak in the WAXS-diffractiogram. Hence, it is not clear, which of the both contributes to the widening in which extent. It is presumed that the piezoelectric effect in wood is mainly effecting the van-der-Waals binding within the cellulose crystal (Pizzi & Eaton, 1984) which indicates that the extension of the crystal will likely occur in (120) layer. The (012) layer in opposite, will be harder to deform since the longitudinal axis of the molecule is locked by covalent and glycosidic bonds (Fengel & Wegener, 1989).

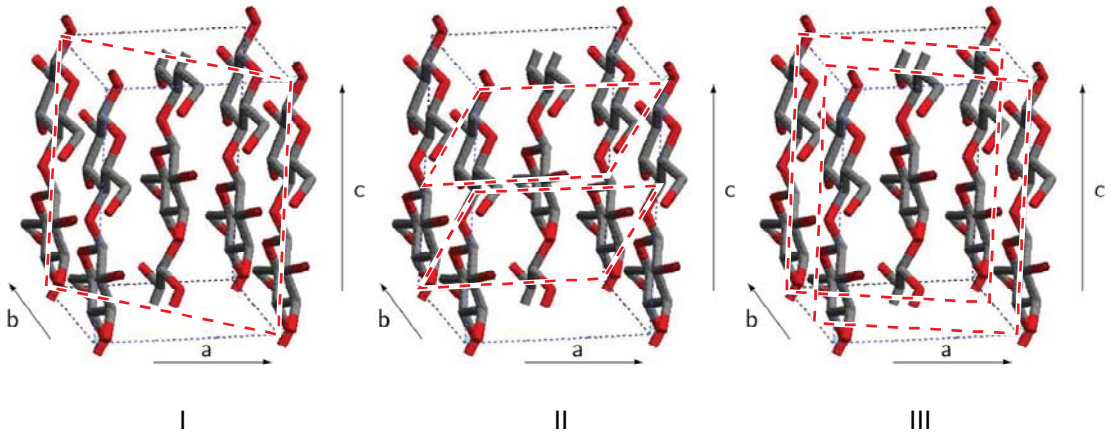

Figure 42: Shows the reflection lattices determined by the WAXS measurements. The left cellulose peak in the WAXS diffractiogram (15.23-19.73° Bragg angle) depicts the (110) layer and is shown in picture I. The second peak (20.42-25.61) depicts both the (012) and (120) layers (shown in picture II and III). Images of the unit cell were taken from (Kölln, 2004).

If a shear-piezoelectric effect would have been present, the unit cells had shown a shift in the orientation of the longitudinal axis. The scattering image was analyzed in that regard, too, but no hint of such a change in the crystallites orientation could be found. Keeping this in mind, following conclusions can be drawn:

Wood samples

- The cellulose I crystallite widens when exposed to an electric field. This is a clear evidence for a piezoelectric effect.

[11] The small increment that was observable can be explained with a possible alteration of the distance of the specimen to the x-ray detector.

- The effect occurs mainly parallel to the crystals longitudinal axis which means that eventually the wood itself widens perpendicular to the grain.
- No effect occurs that would change the crystals orientation. Hence the theory that a converse shear piezoelectric effect would be present seems to be rejected.

Cellulose-foil samples

- No effect in any orientation could've been detected.
- The cellulose foils still showed a reaction in the mechanical measurement, though. This means that either the WAXS method is not accurate enough to detect that small incremental shifts of the cellulose II crystals or another principle of reaction is present that cannot be unveiled by the means of wide angle x-ray scattering.

5.3. Further Research

The research presented in this thesis can only be a starting point on the way of fully understanding the converse piezoelectric effect in wood. The results are interesting, and promise more findings with ongoing into-depth as well as broader investigation of the relationship between wood and an electric field. Below, some research suggestions following this initial work shall be outlined:

5.3.1. Test Series

For statistically significant conclusions, a substantial amount of specimens have to be investigated. Those test series should be able to allow calculation of the displacement depending on:

- *The amplitude of the electric field*

  Until now, only three different voltages have been applied on one sample. This was due to restrictions of the equipment. With a power supply that allows constant variation of the voltage, the piezoelectric reaction on the amplitude of the electric field could be determined much more accurately.

- *The fiber angle*

  Results show a very clear dependence on the fiber angle. Cutting and measuring several samples in different fiber orientations from on sheet of wood would allow to determine an accurate correlation function.

- *The thickness of the sample*

  How deep can an electric field penetrate wooden matter and cause a piezoelectric effect? This could be answered by testing several samples from the same piece of wood with increasing thickness.

- *The micro fibril angle (only for wood samples)*
  Assumed, that the piezoelectric effect is caused by cellulose crystallites it should be dependent on the MFA. Testing samples with different MFAs would verify this theory.

5.3.2. Influence of Polarization

In the course of the mechanical measurements, the polarization was changed for some specimens. The wood samples did not show any difference in the reaction. The cellulose foils, though, appeared to have an altered reaction on the applied electrical field. The differences were rather small and thus not very significant. Deeper research in that occurrence could help understanding the differences in the piezoelectric response for cellulose I and cellulose II crystals.

5.3.3. Comparison of the Direct and Converse Piezoelectric Effect

All relevant literature (see chapter 2) was without exception reporting a shear piezoelectric effect, almost exclusively found in experiments analyzing direct piezoelectricity. The findings in this present thesis strongly indicate not a shear piezoelectric effect, but an effect perpendicular to grain.

In theory, the piezoelectric tensor should be the same for the direct and the converse effect (Benes, 2009), but that seems not to apply for the wooden samples. This discrepancy could be unveiled by a specimen that is analyzed in both principles, the direct and the converse piezoelectric effect. Therefore several thin (e.g. 0.2 mm) wood samples shall be cut in different fiber angles out of the same piece of wood. Additional to the converse experiments that can be carried out just like shown in this thesis, the specimens can be loaded in tension before they’re coated with conductive paint and the occurring electric field shall be measured. The amplitude of the piezoelectric response (direct and converse) can then be put in relation for each fiber angle.

6. Bibliography

Bazhenov, V. A. (1961). *Piezoelectric Properties of Wood.* New York: Consultants Bureau.

Benes, E. (2009). *Piezoelectric Materials.* Vienna: Institut für allgemeine Physik, Technische Universität Wien.

Bower, D. I. (2002). *An Introduction to Polymer Physics.* Cambridge, UK: Cambridge University Press.

Bruker ASX. (2009). Retrieved June 7, 2009, from A Big-Anlge View of Small Angle Measurements: SAXS Techniques: http://www.bruker-axs.de/fileadmin/user_upload/pdf_pool/BAXS/Technical%20Documents/Products%20XRD/Presentations/Bruker_AXS_SAXS_Webinar_XRD.pdf

Fengel, D., & Wegener, G. (1989). *Wood - Chemistry, Ultrastructure, Reactions.* Berlin, New York: Walter de Gruyter.

Fukada, E. (1955). Piezoelectricity of Wood. *Journal of the Physikal Society of Japan , 10* (2), pp. 149-154.

Galligan, W. L., & Bertholf, L. D. (1963). Piezoelectric Effect in Wood. *Forest Product Journal , XIII* (12), pp. 517-524.

Greer, L., & Pemberton, S. R. (2009). *The structure and mechanical behaviour of wood*. Retrieved June 28, 2009, from http://www.doitpoms.ac.uk/tlplib/wood/printall.php

Kelso, P. W. (1969). *Piezoelectric Effect in Wood.* Master Thesis, Washington State University, Pullman.

Kim, J., Yun, S., & Ounaies, Z. (2006). Discovery of Cellulose as a Smart Material. *Macromolecules* (39), pp. 4202-4206.

Klemm, D., Heublein, B., Fink, H. P., & Bohn, A. (2005). Cellulose: Fascinating Biopolymer and Sustainable Raw Material. *Angewandte Chemie Internationale Edition* (44), pp. 3358-3393.

Kölln, K. (2004). *Morphologie und mechanische Eigenschaften von Zellulosefasern.* Dissertation, Mathematische-Naturwissenschaftliche Fakultät, Christian-Albrechts-Universität, Kiel.

Nakai, T., Igushi, N., & Ando, K. (1998). Piezoelectric behavior of wood under combined compression and vibration stresses - Relation between piezoelectric voltage and microscopic deformation of a Sitka spruce. *J Wood Sci* (44), pp. 28-34.

Niemz, P., Emmler, R., Pridöhl, E., Fröhlich, J., & Lühmann, A. (1994). Vergleichende Untersuchungen zur Anwendung von piezoelektrischen Untersuchungen und Schallemissionssignalen bei der Trocknung von Holz. *Holz als Roh- und Werkstoff* (52), pp. 162-168.

Nishiyama, Y., Sugiyama, J., Chanzy, H., & Langan, P. (2003). Crystal Structure and Hydrogen Bonding System in Cellulose. *J. Am. Chem. Soc. , 125(47)* , 14300-14306.

Pizzi, A., & Eaton, N. (1984). Correlation between the Molecular Forces in the Cellulose I Crystal and the Piezoelectric Effect in Wood. *Holzforschung Holzverwertung* (30), pp. 12-14.

Pizzi, A., & Knuffel, W. (1986). The Piezoelectric Effect in Structural Timber. *Materialforschung* (3), pp. 157-162.

Prior, M. (2009). *Röntgenbeugung*. Retrieved Juni 8, 2009, from https://lp.uni-goettingen.de/get/text/1526

Raven, P. H., Evert, R. F., & Eichhorn, S. E. (2006). *Biologie der Pflanzen.* Berlin: de-Gruyter.

Wada, M., Sugiyama, J., & Okano, T. (1993). Native Cellulose on the Basis of Two Crystalline Phase (1α/1β) System. *Journal of Applied Polymer Science* (49), pp. 1491-1495.

Zimmermann, T., Pöhler, E., & Geiger, T. (2004). Cellulose Fibrils for Polymer Reinforcement. *Advanced Engineering Materials , 9* (6), pp. 754-761.